The Thesis committee for Devin Scott Fraley

Certifies that this is the approved version of the following thesis:

A Radiolabeling Approach to Purinoceptor-like Receptor Identification in Plants and Evidence for Apyrase (APY1 and APY2) Regulation of Stomatal Aperture in *Arabidopsis*

APPROVED BY

SUPERVISING COMMITTEE:

Supervisor: _____

Stanley J Roux

_____

Gregory B Clark

A Radiolabeling Approach to Purinoceptor-like Receptor Identification in Plants and Evidence for Apyrase (APY1 and APY2) Regulation of Stomatal Aperture in *Arabidopsis*

by

Devin Scott Fraley, B. S.

Thesis

Presented to the Faculty of the Graduate School

of the University of Texas at Austin

in Partial Fulfillment

of the Requirements

for the Degree of

Master of Arts

The University of Texas at Austin

December 2010

To my loving wife, Anna

Acknowledgements

I would like to thank Dr. Stan Roux for his interest and key role in my success. Dr. Roux welcomed me to frequent discussions about my experiments or results and provided invaluable guidance and support. He invested time, care, and patience to ease me through numerous frustrating research experiences. Dr. Roux served as a superb mentor, educating me on matters directly relevant to my research but also about science from a general perspective. I appreciate our enlightening talks, his extensive knowledge, and his concern for his students.

I would also like to thank Dr. Greg Clark as a secondary mentor and collaborator. Dr. Clark was essential to familiarizing me to the lab when I first started and has since made himself available to me for help or concerns. It has also been a pleasure to combine efforts with Dr. Clark on stomata work.

Much of my success has also been the result of the assistance and friendship of others in Dr. Roux's Lab including Sonya Chiu, Minhui Lim, Jian Yang, Dr. Jian Wu, Julia Kays, Jonathan Torres, and Parag Sevak. I am thankful for their direct help with techniques and suggestions, but also the long stress-relieving chats and pointless debates we shared.

Beyond the lab, I must thank my wife, Anna, for her constant love, encouragement, and support. I appreciate her hard work, company on long drives to campus for experiments at night, and patience during my occasional sleepless nights. I

also thank my parents, Jim and Jennifer, for their love and encouragement, and hold them responsible for igniting my creativity and initial interest in science and academia.

A Radiolabeling Approach to Purinoceptor-like Receptor Identification in Plants and Evidence for Apyrase (APY1 and APY2) Regulation of Stomatal Aperture in *Arabidopsis*

by

Devin Scott Fraley, M.A.

The University of Texas at Austin, 2010

SUPERVISOR: Stanley J Roux

Adenosine triphosphate (ATP) is well recognized for its role as the primary cellular energy currency. However, studies dating back to 1929 have reshaped our understanding of ATP as not only an energy source, but also as a signaling agent. Among the most important of these discoveries are animal purinergic receptors (P2X and P2Y receptors) that perceive extracellular ATP (eATP), primarily in the nervous system. Though eATP is an established receptor agonist in animals and applied poorly hydrolyzable ATP analogs have numerous effects on growth in plants, eATP is not widely accepted as a signal in plants where no purinoceptor has been identified.

Here, enriched outside-out plasma membrane vesicles were isolated and proteins labeled with a radioactive ATP analog ($8N_3ATP[\alpha^{32}P]$) to identify a putative purinoceptor-like receptor. We used etiolated seedlings to capture proteins from plant tissue that was actively growing and used sodium carbonate washes to separate peripheral

and integral membrane proteins. With this method, we have generated lists of plasma membrane ATP binding proteins, and therefore possible eATP receptors.

Ectoapyrases are phosphohydrolases thought to regulate eATP in both animals and plants. Here, we also investigated the expression and role of the candidate ectoapyrases AtAPY1 and AtAPY2 in guard cells and stomatal responses. AtAPY1 and AtAPY2 transcript and protein expression was confirmed in guard cells. Early genetic studies using an *apy2* knock out with induced RNAi-silencing of *APY1* suggest a role for these apyrases in stomatal regulation. In response to treatment with five hours light, the apyrase-suppressed line features wider stomatal aperture when compared to WS wild-type.

Table of Contents

List of Figures

Chapter 1: Introduction

Like animal cells, plant cells must be able to sense and respond to environmental and endogenous stimuli. By doing so, plants can adapt to wounding, water stress, varying light quality, and touch despite their sessile state. These stimuli, perceived by plants electrically, mechanically, or chemically, initiate signal transduction pathways where secondary messengers are activated to evoke a specific response.

Like animals, plants use extracellular molecular signals, or hormones, to allow intercellular communication. While some plant hormones, such as auxin, have been recognized since the early 1900s (Kogl et al. 1931), the past thirty years have involved the discovery of exciting new hormones including brassinosteroids (Grove et al. 1979) and the identification of long unknown hormone receptors including that for abscisic acid (ABA) (Pandey et al. 2009). Among these new discoveries also exists evidence for extracellular ATP (eATP) as a signaling agent in plants. However, despite current evidence, eATP signaling in plants remains poorly understood relative to animal literature where a role for eATP has been well defined.

The effects of applied adenine compounds, adenosine and adenosine monophosphate (AMP), were first observed in the animal heart in 1929 (Drury and Szent-Györgyi). Fifteen years after the original discovery of adenosine responses, it was found that applied adenosine triphosphate (ATP) altered muscle responses to acetylcholine (Buchthal et al. 1944) and had other effects on the spinal cord (Buchthal et al. 1947). eATP was later proposed to act as a neurotransmitter (Burnstock et al. 1970).

Since then, the understanding of eATP signaling in animals has flourished, including the development of downstream signal transduction pathways and the identification of receptors for eATP coined "purinergic" receptors (Burnstock 1972).

In animals, eATP initiates signal transduction pathways when it binds to transmembrane purinergic receptors. These receptors are responsible for the reception of not only ATP, but also adenosine, AMP, and ADP. As a result, the purinergic receptors are divided into two families: P1 and P2 receptors (Burnstock 1980). P1 receptors bind adenosine and AMP while P2 receptors bind ADP, ATP, and other nucleoside di- and triphosphates (Burnstock and Kennedy 1985). The P2 receptors also fall into two distinct categories; P2Y receptors are G-protein coupled receptors (reviewed by Abbracchio et al. 2006), while P2X receptors are ligand-gated cation channels (reviewed by North 2002).

Though animal purinergic receptors are well characterized, including the recent development of a crystal structure for a P2X receptor (Kawate et al. 2009), no receptor for eATP has been identified in plants. Alignments of animal P2X receptors have helped identify putative purinoceptors with strong sequence similarity in the green algae *Ostreococcus tauri* (Fountain et al. 2008), but alignments have proved unsuccessful in identifying a receptor in vascular plants. The inability to find a putative purinoceptor is likely one contributing factor to hesitations accepting eATP signaling in plants.

Though a purinoceptor has not been discovered in higher plants, many studies support a role for eATP in plants. Dating back to the 1970s and 1980s, applied ATP in millimolar concentrations increased K^+ uptake in leaf cells (Luttge et al. 1974), micromolar concentrations stimulated Venus'-flytrap closure (Jaffe 1973) and millimolar

concentrations induced stomatal opening (Nejidat et al. 1983). However, due to either the high concentrations used or the known role of ATP as a cellular energy currency, it was reasoned that these effects were the result of excess energy provided by ATP that could be taken up by cells.

Recent studies have considered downstream signal transduction pathways in animals where applied ATP causes transient increases in $[Ca^{2+}]_{cyt}$ (Charest et al. 1985). In *Arabidopsis*, nanomolar to low micromolar concentrations of ADP, ATP, and poorly hydrolyzable ATP analogs applied to seedlings and roots were shown to cause an elevation in $[Ca^{2+}]_{cyt}$ (Demidchik et al. 2003, Jeter et al. 2004). Applied poorly hydrolyzable ATP (ATPγS or αβmeATP) upregulates transcripts for MAP kinases, genes involved in ethylene synthesis (Jeter et al. 2004), and ROS secondary messengers (Song et al. 2006, Kim et al. 2006) including hydrogen peroxide (Wu et al. 2008) and nitric oxide (Foresi et al. 2007, Wu et al. 2008).

In addition to inducing secondary messengers and altering gene expression, applied ATP has several physiological effects in plants. Early studies in *Arabidopsis* showed eATP is involved in toxin resistance (Thomas et al. 2000), and can inhibit both root gravitropism (Tang et al. 2003) and pollen germination (Steinebrunner et al. 2003). Later studies with poorly hydrolyzable ATP and ADP analogs, applied in micromolar concentrations, found both to affect pollen germination, pollen tube elongation (Reichler et al. 2009), cotton fiber growth (Clark et al. 2010a), and root hair growth in a dose-dependent manner (Clark et al. 2010b).

Though ATP is valuable to the cell as an energy source, it must be secreted or otherwise released from the cell for eATP to induce a response. Osmotic (Mitchell 2001), mechanical (Romanello et al. 2001) and other stresses result in ATP export from animal cells. Studies in plants have used a luciferin-luciferase assay (Jeter et al. 2004) and radiolabeling (Chivasa et al. 2005) to report plant cell ATP efflux. Wounding (Song et al. 2006), exocytosis (Kim et al 2006), mechanical stimulation, and osmotic stress (Jeter et al 2004**,** Kim et al 2009) are all proposed mechanisms for release of ATP from plant cells. To determine if ATP was released from plant cells under resting conditions and present extracellularly, a hybrid cellulose-binding luciferase gene was used to observe that ATP is heavily secreted from growing tissues (Kim et al. 2006).

As it does with all signaling agents, a cell must regulate levels of eATP. Ectoapyrases are di- and tri-phosphatases at the plasma membrane responsible for regulating eATP in animals (Zimmerman 2001). High efficiency, low substrate specificity, and protein structure grant ectoapyrases this unique physiological role amongst other phosphatases (reviewed by Komoszynski and Wojtczak 1996). Apyrases sharing several conserved domains with those in animals have also been identified in plants (Handa and Guidotti 1996).

In *Arabidopsis thaliana*, there are two apyrases thought to act as ectoapyrases: AtAPY1 and AtAPY2 (Wu et al. 2007). APY1 and APY2 are most heavily expressed in growing tissues (Wu et al. 2007), similar to the regions where eATP secretion was reportedly strongest (Kim et al. 2006). Single knockout *apy1* and *apy2* mutants do not exhibit an easily observed phenotype, likely explained by redundancy and the 87%

sequence similarity between them. Since APY1 and APY2 act mostly redundantly, double knockouts were generated for genetic studies of apyrase in *Arabidopsis*. This approach was unsuccessful but made it evident that double knockouts resulted in inhibition of pollen germination (Steinebrunner et al. 2003).

An *apy1/apy2* double knockout with *APY1* or *APY2* under a pollen specific promoter was used to allow pollen to germinate and fertilize eggs. The embryos developed normally, the seeds germinated, and the resulting dwarf seedlings featured a lack of true leaves, lacked properly developed roots, and caused seedling lethality amongst other abnormalities (Wolf et al. 2007). To better understand the effects of APY1 and APY2 on growth, *apy2* mutants with inducible RNAi constructs targeting *APY1* were developed. When induced, phenotypes included 70% inhibition of hypocotyl growth after 3.5 days and approximately 70% inhibition of root growth after 6 days (Wu et al. 2007).

Studies suggest that APY1 and APY2 function extracellularly and act through the hydrolysis of ATP and ADP. Specific anti-apyrase antibodies, added to pollen germination medium, inhibit pollen germination as consistent with *apy1*/*apy2* double knock-out mutant phenotype (Wu et al. 2007). Furthermore, the concentration of eATP was found to rapidly and transiently increase in the pollen germination medium in the presence of anti-apyrase antibodies (Wu et al. 2007). As antibodies are not thought to cross the plasma membrane, this evidence would support that APY1 and APY2 act in the extracellular matrix, and the increase in eATP confirms that they function in the hydrolysis of ATP. Similar results have also been found in cotton fibers where the

addition of anti-apyrase antibodies reduces cotton fiber growth and increases the concentration of eATP in the medium (Clark et al. 2010a).

Considering that APY1 and APY2 are strongly expressed in expanding cells, guard cells have generated interest for further apyrase studies. Two bean-shaped guard cells in the leaf epidermis surround each stoma; a pore responsible for transpiration and the diffusion of CO_2 into the leaf for photosynthesis. The size of the pore, or stomatal aperture, is regulated by the turgidity of the guard cells—the stomata are open when the guard cells are swollen with water and closed when they are not. Turgidity is controlled by fluctuations in the osmotic potential of guard cells, signaled by stimuli including blue light and abscisic acid (ABA) to cause opening and closure respectively.

To cause stomatal closure, ABA induces an intracellular spike in Ca^{2+} (McAinsh et al. 1990) that blocks inward K^+ channels and activates Ca^{2+}-gated anion channels, thereby depolarizing the guard cell plasma membrane (Schroeder and Hagiwara 1989). The depolarization is responsible for K^+ efflux by activating outward-directed K^+ channels and deactivating inward-directed K^+ channels (Shroeder et al. 1987). The movement of anions and K^+ out of the guard cells decreases the water potential outside of the cell, resulting in the outward movement of water that leaves the guard cells flaccid and stomata closed.

Many signal transduction events downstream of ABA have been elucidated in recent years. Early studies suggest a role for hydrogen peroxide (H_2O_2) (McAnish et al. 1996) and nitric oxide (NO) (Garcia-Mata et al. 2001, Desikan et al. 2002) in stomatal closure. H_2O_2 causes an increase in $[Ca^{2+}]_{cyt}$ (McAnish et al. 1996) and can be generated

in guard cells under a variety of stresses (Neill et al. 2002). It has also been established that ABA induces H_2O_2 generation in the pathway to closure (Pei et al. 2000). ABA also leads to nitric oxide (NO) accumulation in guard cells, and the use of NO scavengers inhibits stomatal closure in response to ABA (Neill et al. 2002, Desikan et al. 2002, Garcia-Mata et al. 2002). Neill et al. (2008) summarized these and other known components of the ABA signaling pathway for stomatal closure were summarized in a model.

When guard cells swell or shrink, the surface area of their plasma membrane changes to accommodate the fluctuating cell volume (Shope et al. 2003). As exocytosis and stretching of the plasma membrane were previously shown to act as export pathways for ATP from a cell, it was hypothesized that ATP is passively released from guard cells during stomatal opening. Furthermore, applied ATP promotes ROS and NO production in other tissues as previously described (Song et al. 2006, Kim et al.2006, Foresi et al. 2007, Wu et al. 2008, Clark et al. 2010b). Because H_2O_2 and NO play known roles in stomatal closure in response to ABA and stressors (Neill et al. 2008), it was hypothesized that ATP secreted from expanding guard cells may be perceived by guard cells to resist further opening or induce closure.

These hypotheses were not addressed in this thesis, but preliminary data from the Roux lab (Clark et al., unpublished) suggests that high concentrations of applied ADPβS and ATPγS (poorly hydrolyzable analogs) indeed promote stomatal closure in the light in a dose-dependent manner. Surprisingly, low concentrations of ADPβS and ATPγS also affected stomata by promoting their opening in the dark in a dose-dependent manner.

Thus far, these responses have been shown to be inhibited by the animal purinoceptor inhibitor PPADS, consistent with the hypothesis that the responses observed in guard cells are the result of agonist binding to an unknown plant purinoceptor.

If eATP has a signaling role in guard cells, this suggests that APY1 and APY2 may be expressed in guard cells to regulate the eATP signal. Preliminary APY1 and APY2 promoter:GUS expression supports that *APY1* and *APY2* are expressed in guard cells of open stomata (Steinebrunner, unpublished). Therefore, it was hypothesized that AtAPY1 and AtAPY2 are expressed in guard cells and act to reduce eATP concentrations thereby promoting stomatal opening.

Here, two different aspects of eATP signaling in plants are addressed. One goal of my research was to identify a purinoceptor in *Arabidopsis* by radio-labeling outside-out plasma membrane proteins. Though no putative receptor has been identified, the results described in this thesis may help guide future experiments. The second focus of my research was to examine a potential role for APY1 and APY2 in *Arabidopsis* guard cells. Here, I address the expression of APY1 and APY2 in guard cells and describe an early genetic approach to understanding their role in guard cells.

Chapter 2: Plasma membrane radiolabeling approach to identifying a plant purinoceptor-like receptor

Chapter 2.1: Materials and Methods

2.1.1 Dark-grown (etiolated) seedling plasma membrane radiolabeling

Etiolated Plant Material:

Approximately 50-70 g of plant tissue from 3.5 day old etiolated seedlings (per experiment) was used to isolate sufficient plasma membrane. 3 g seeds from *Arabidopsis thaliana,* ecotype Col-0, were sterilized by soaking in ddH_2O for 20 min, then 80% ethanol for 1 min, and then 20% bleach for 2 min. Seeds were washed 5 times with autoclaved ddH_2O and plated on filter paper placed on a Murshige-Skoog medium across four 15 mm petri plates (no sucrose, pH 5.7-6.0, 1.2% agar). The plated seeds were vernalized for 4 days at 4^{o}C in the dark. After 4 days, the seeds were placed in the light for 6 h at 25^{o}C. Plates with seeds were then wrapped in foil and placed flat (horizontally) at 25^{o}C for 3.5 days.

Etiolated Seedling Plasma Membrane Isolation:

Samples enriched with outside-out plasma membrane vesicles were obtained following the protocol described by Larsson et al. (1994). Between 30-70 g of etiolated seedlings was blended in a Waring blender for 5 min on the low setting in 50 ml of homogenization buffer (330 mM sucrose, 50 mM MOPS, 5 mM EDTA, 5 mM ascorbic acid, 0.2% casein hydrolysate, 0.6% PVPP, pH 7.5 with KOH, 5 mM fresh DTT, and 1x SIGMA*FAST* Protease Inhibitor Tablets). The blended plant material was then filtered

through Miracloth and the liquid fraction was collected. The liquid fraction was then centrifuged at 10,000 g (JA20 rotor -1 compensation), 4^{o}C for 25 min, thereby pelleting plastids and mitochondria. After the first centrifugation, the supernatant was extracted and spun at 60,000 g (Sorvall RM28 rotor), 4^{o}C for 80 min. Supernatant was decanted to leave pellets consisting of membrane, and the pellets were resuspended in Resuspension Buffer (330 mM sucrose, 5 mM potassium phosphate, 0.1 mM EDTA, pH 7.8) so that the final weight of the resuspended pellet was 24 g.

Two-phase partitioning:

To each of eight 30 ml glass tubes, 18 g of bottom phase mixture (20% (w/w) Dextran T500, 40% (w/w) PEG 3350, 2.0 M sucrose, 2.0 M KCl, and 0.2 M potassium phosphate) was added. To four of these tubes with bottom phase, 6 g of Resuspension Buffer (with fresh 1 mM DTT and 1x protease inhibitor added) was gently layered on top of the bottom phase to form two-phase solutions.

All four two-phase tubes were mixed by inversion 30 times, and when mixed, they were centrifuged at 1000 g (JS 13.1 rotor), 4^{o}C for 5 min. This centrifugation resulted in two distinct phases--the upper phase was stored in a beaker and the bottom phase saved in the same four glass tubes. 6 g plant material (from earlier resuspended pellet) was then layered on the bottom phase of the second set of tubes (unused). These tubes were also mixed by 30 inversions and centrifuged at 1000 g (JS 13.1 rotor), 4^{o}C for 5 min. 90% of the upper phase with plant material was siphoned off, layered on the bottom phase from the first set of tubes (clear, without plant material) and then inverted and centrifuged as described above. The resulting upper phase was saved for

ultracentrifugation. This procedure was repeated with 12 g (two tubes worth) of the upper phase previously stored, which did not contain plant material, by mixing it with both bottom phase sets from which plant material had previously been mixed with. The resulting upper phase was also saved for ultracentrifugation to increase yield from the 10% of upper phase not previously collected after each centrifugation and from outside-out plasma membrane vesicles trapped in the bottom phase.

The upper phase containing the outside-out membrane vesicles was diluted with sufficient Resuspension buffer to fill four ultracentrifuge tubes. These tubes were centrifuged in at 100,000 g (Sorvall RM28 rotor) for 1.5 h. The resulting pellets containing enriched outside-out plasma membrane vesicles were resuspended with cut tips in 50 µl Radiolabeling Buffer and the Bradford Assay (Bio-Rad) was used to determine the protein yield using bovine serum albumin (BSA) as a standard.

Radiolabeling:

6 µCi $8N_3ATP[\alpha^{32}P]$ was added for every 125 µg protein to the plasma membrane sample. The sample was inverted 10x to mix and photoilluminated with UV light (254 nm, 4000 µW) for 60 sec. 10 mM DTT was then immediately added to quench the crosslink reaction and the labeled protein was snap-frozen with liquid nitrogen.

2-D PAGE, autoradiography, and LC-MS-MS Analysis:

Labeled plasma membrane from four separate plasma membrane isolations was sent to Kendrick Laboratories Inc. where the protein was later combined and concentrated. Two-dimensional polyacrylamide gel electrophoresis (2-D PAGE), performed by Kendrick Laboratories, Inc., was used to separate proteins from the

outside-out plasma membrane enriched sample that was labeled with $8N_3ATP[\alpha^{32}P]$. In addition to the separation by mass (kD) as is done in 1-D SDS-PAGE, proteins were also separated by isoelectric point. Samples were boiled in SDS and run in a tube gel using the carrier ampholine method which stripped SDS for isoelectric focusing (Anderson and Anderson 1977). The tube gel was then sealed to a stacking gel for protein separation by molecular weight. The resulting 2-D gel was Coomassie stained and exposed to x-ray film for 16 days at -80^{o}C to develop an autoradiogram. The autoradiogram was overlaid with the Coomassie-stained 2-D gel and spots were cut out based on molecular weight and recommendations from Kendrick Labs. Once cut out, proteins were analyzed with liquid chromatography-tandem mass spectrometry (LC/MS-MS) by Kendrick Laboratories, Inc.

2.1.2 Light-grown seedling plasma membrane radiolabeling and $NaCO_3$ wash

Light and Liquid-Grown Plant Material:

Approximately 150 g of light grown seedlings were used to isolate sufficient plasma membrane in each experiment. 1 g seeds from *Arabidopsis thaliana*, ecotype Col-0, was divided into five separate 15 ml tubes (each with 0.2 g seeds). In these tubes, seeds were sterilized by soaking in ddH_2O for 3 h and then 50% bleach for 20 min. Seeds were centrifuged and rinsed 5 times with freshly autoclaved ddH_2O. Each 0.2 g aliquot of sterilized seeds was transferred to separate 1 L flasks containing 500 ml freshly autoclaved liquid media (2.15 g/L MS, 3% sucrose, pH 5.7). Seeds were vernalized in liquid media for 3 days at 4^{o}C and then grown in the light on a rotator (85 RPM) for 10 days.

Isolation and Radiolabeling of plasma membrane from light-grown seedlings

Enriched outside-out plasma membrane vesicles were isolated as described by Larsson et al (1994). 150 g starting material was blended in a Waring blender and all other steps were completed as previously described from etiolated seedlings. Resulting plasma membrane samples were also radiolabeled with $8N_3ATP[\alpha^{32}P]$ as earlier described.

Sodium Carbonate Wash

Labeled plasma membrane samples were washed with 0.8 ml of 0.1 M sodium carbonate (pH 11.5) on ice for 30 min. Samples were then centrifuged at 136,000 g (Beckman TL-100 TLS 55 rotor) resulting in a soluble and insoluble fraction. The soluble fraction was removed and placed in a separate tube where it was brought to pH 7 with 0.5 M MES. Both soluble and insoluble fractions were then snap-frozen with liquid nitrogen.

2-D PAGE, autoradiography, and LC/MS-MS analysis

Labeled soluble and insoluble fractions were sent to Kendrick Laboratories Inc. where all soluble fractions were combined, insoluble fractions were combined, and proteins were concentrated. Kendrick Labs separated soluble protein fractions with standard 2-D PAGE and insoluble protein fractions with the 2-D PAGE carrier ampholine method previously described with etiolated seedlings. Kendrick Labs developed an autoradiography for both soluble and insoluble fraction 2-D gels, and cut out and sequenced spots of interest with LC/MS-MS.

Chapter 2.2: Results

$8N_3ATP[\alpha^{32}P]$ radiolabel analysis of enriched outside-out plasma membrane vesicle proteins isolated from etiolated tissue

Enriched outside-out plasma membrane vesicles were isolated from etiolated *Arabidopsis* seedlings and proteins were labeled with $8N_3ATP[\alpha^{32}P]$ as described in Materials and Methods. As indicated by the Bradford Assay, 1045 µg total protein was combined across four separate plasma membrane isolations yielding 267 µg, 286 µg, 164 µg, and 328 µg protein (each radio-labeled individually).

The labeled plasma membrane proteins were separated by 2-D gel electrophoresis by Kendrick Laboratories, Inc. who also developed an autoradiogram of the 2-D gel. The autoradiogram had 11 spots (labeled A-K), varying in molecular weight, showing that $8N_3ATP[\alpha^{32}P]$ bound to many plasma membrane proteins. Of these spots, A, D, E, G, and I were sequenced with Liquid Chromatography/Tandem Mass Spectrometry (LC/MS-MS) by Kendrick Labs, while spots at lower molecular weight were not.

Spot A revealed peptides from 26 different proteins in the corresponding excised gel (Figure 4.1). For spots D, E, G, and I, one predominant protein was sequenced from each spot (Figure 4.3). Some proteins that were sequenced have been previously identified as plasma membrane proteins including fasciclin arabinogalactan-protein (FLA2:At4g12730) and calmodulin-domain protein kinase (CPK9:At3g20410) (Alexandersson et al. 2004), but other sequenced proteins including rubisco large subunit (AtCg00490) and 60S ribosomal protein L8-1 (AT2G18020) are known contaminants indicating an impure protein sample.

A similar approach to identifying a purinoceptor in plants using two-phase plasma membrane purification from light grown seedlings was used by Timothy Butterfield of Dr. Stan Roux's lab in 2006. He radiolabeled enriched outside-out plasma membrane proteins with both $8N_3ATP[\gamma^{32}P]$ and $8N_3ATP[\alpha^{32}P]$ (Butterfield 2007). Overlapping proteins sequenced from Timothy Butterfield's experiments and the one described here include: MAP3K-like protein kinase, phospholipase C (PLC2), and annexin 2 (AnnAt2). Other overlapping subfamilies included fasciclin-like (FLA) and patellin (PATL) proteins.

$8N_3ATP[\alpha^{32}P]$ radiolabel analysis of soluble and insoluble protein fractions from enriched outside-out plasma membrane vesicles

Enriched outside-out plasma membrane vesicles were isolated from liquid grown *Arabidopsis* seedlings in continuous light as described in Materials and Methods. As indicated by the Bradford Assay, 506 µg total protein was combined across four separate plasma membrane isolations yielding 136 µg, 256 µg, 48 µg, and 66 µg protein (each radio-labeled individually with $8N_3ATP[\alpha^{32}P]$). After radiolabeling, a soluble protein fraction and insoluble protein fraction was obtained by washing the labeled plasma membrane proteins with sodium carbonate.

The soluble and insoluble fractions with labeled plasma membrane proteins were separated on two 2-D gels Coomassie-stained by Kendrick Laboratories, Inc. who also developed autoradiograms for both gels (Figure 4.2). The autoradiogram of the gel separating the soluble fraction proteins had 11 spots (labeled A-J, and a "?" for a less bold spot), varying in molecular weight, showing that $8N_3ATP[\alpha^{32}P]$ bound to many

peripheral membrane proteins. Of these spots, proteins from B, E, I, and "?" were cut out and sequenced with LC/MS-MS by Kendrick Labs, while other spots were not (Figure 4.2).

As in the previous experiment described where plasma membrane was isolated from etiolated seedlings, at some spots (I, B, "?") there were few different proteins sequenced, while at other spots (E), at least 1 unique peptide was identified from each of 8 different proteins (Figure 4.4). Many of the proteins sequenced have been previously identified in plasma membrane protein isolations including ATMS1 (At5g17920), SKU5 (At4g12420), and ASNAP (At1g56190) (Alexandersson et al. 2004) and no certain non-plasma membrane contaminants were sequenced indicating that the pure plasma membrane isolation used was relatively pure.

A similar approach to radiolabeling membrane proteins was performed by Timothy Butterfield (2007) and as previously described with etiolated seedlings in this thesis. Overlapping proteins between the soluble fraction and Timothy Butterfield's work include patellin 1, phospholipase C, and annexin 2 while overlapping subfamilies also include fasciclin-like proteins. Overlapping proteins between the soluble fraction and the plasma membrane proteins isolated from etiolated seedlings described previously in this thesis include cold-regulated 47 (COR47), brassinosteroid signaling kinase 1 (BSK1), annexin 2 (ANNAT2), phospholipase C (PLC2), fasciclin-like arabinogalactic protein 13 (FLA13), and aldehyde dehydrogenase 4 (ALDH3H1). Proteins in common between Timothy Butterfield's work and both labeling experiments described here include AnnAt2, PATL1, and PLC2.

The autoradiogram of the gel with the radiolabeled insoluble fraction had less spots than the soluble fraction did, with four spots in total as identified by Kendrick Labs (labeled H, I, J, and K) (Figure 4.2). Spots H, I, and J were sequenced with LC/MS-MS by Kendrick Labs and the most prevalent proteins were recorded (Figure 4.4). None of the proteins sequenced were in common with the proteins identified in earlier labeling experiments.

Chapter 3: Expression and role of APY1 and APY2 in stomatal responses

Chapter 3.1: Materials and Methods:

3.1.1 Semi-quantitative PCR analysis of guard cell *APY1* and *APY2* transcript expression

Plant Material:

Approximately 80 Col-0 and WS plants (in separate experiments) were grown on soil for 2-3 weeks in continuous light at 19-21^{o}C until the basal leaves matured. 100 basal leaves were excised from approximately 70 of these plants and guard cell protoplasts were isolated from them following an overnight method previously described, omitting the Histopaque purification steps (Pandey et al. 2002). This procedure yielded approximately 0.1 g wet weight of enriched guard cell protoplasts. About 10 remaining intact plants were also placed in the dark for 12-13 hours (parallel to the light conditions of the protoplast sample) for plant material from whole leaves.

Transcript Expression:

Total RNA was extracted (Sigma Spectrum^{TM} Plant Total RNA Kit 50 Prep**)** from 0.1 g (wet weight) enriched guard cell protoplasts (at least >50% purity as determined by counting cells on a microscope slide; not quantified with a hemacytometer) and from 0.1 g whole leaves excised from the leftover plants in the dark. Reverse transcription PCR was employed (Invitrogen) to create a cDNA library and *APY1*, *APY2*, and actin primers were used to amplify those transcripts with 25 cycles in the thermal cycler (*APY1* primers

were 5'-GCAGCCGTAACTTGCAATC-3' and 5'-CACAGCGTAATTCTTCGGACC-3', for *APY2* primers were 5'- GCTTTCCCAAATTCACCGT-3' and 5'-CACAGCGTAATTCTTCGGACC-3', and for actin were 5'-AACTCTCCCGCTATGTATGTCGC-3' and 5'-CCATCTCCTGCTCGTAGTCAACA-3'. The amplified cDNA was run on a 1% agarose gel with ethidium bromide and visualized under ultraviolet light.

3.1.2 Western blot analysis of APY1 and APY2 protein expression in guard cells

Western Blot Analysis:

Total protein was extracted from 0.1 g enriched guard cell protoplasts (at least >50% purity) and from 0.1 g of whole leaves excised from leftover plants in the dark. Protein was extracted by grinding tissue in an Eppendorf tube with a pestle in 1 ml of protein extraction buffer: 0.1 M Tris (pH 6.8), 20% glycerol, 5% SDS, 200 mM DTT, 200 µM PMSF, and SigmaFAST™ Protease Inhibitor Cocktail Tablets (used as instructed). After they were ground, the samples were boiled and centrifuged, and the soluble fraction was saved for electrophoresis.

Protein concentration was determined using the Bradford Assay and 20 µg enriched guard cell protein and whole leaf protein was loaded on SDS-PAGE pre-cast gels (BIO-RAD Mini-PROTEAN® TGX™, 10%) along with Precision Plus Standard (BIO-RAD). The gel was run at 60 V (constant voltage) for 10 min through the stacking gel and then at 100 V (constant voltage) until the green pigment front ran off the gel, and the protein was transferred to a nitrocellulose membrane at 50 mA (constant current).

The membrane was blocked with 3% milk in phosphate buffered saline (PBS) and then rinsed with PBS for 2 min. To detect APY, the membrane was submerged in 1% milk in PBS with a 1:1000 dilution of anti-apyrase polyclonal antibodies raised in guinea pig (GP1318) against APY1 that can also recognize APY2. To detect tubulin, the nitrocellulose membrane was submerged in 1% milk in PBS with a 1:2500 dilution of anti-α-Tubulin monoclonal antibodies raised in a mouse (Sigma). Both 1^{o} antibodies probed the membrane overnight (15-20 hours) at 4^{o}C.

The nitrocellulose was then rinsed twice with PBS for 2 min and submerged in the appropriate 2^{o} antibody. For APY detection, a conjugated anti-guinea pig IgG antibody to an infrared dye (Rockland) was diluted 1:5000 in PBS with 1% milk for 2 h and for α-tubulin detection, anti-mouse IgG antibody conjugated to an infrared dye (Rockland) was diluted 1:5000 in PBS with 1% milk for 2 h. After 2 h, membranes were rinsed by submerging in PBS 5 times for 5 min. Signals from target proteins on the nitrocellulose were detected with the Odyssey Infrared Imaging System (Li-Cor Biosciences).

3.1.3 Stomatal responses in apyrase mutants to light and abscisic acid (ABA)

Plant Material:

WS and mutant R2-4A (estradiol-induced RNAi line) *A. thaliana* seeds were planted directly on soil, spaced apart such that only five seeds were planted per pot. Seedlings were grown for about 3 weeks (until the flowering bolt first appeared) in continuous light at 19-21^{o}C. After the plants began bolting, 1 pot per stomatal measurement experiment of each line of plants (WS and R2-4A) was moved to a separate tray to be treated with the inducer, estradiol. 40 mM estradiol in DMSO was diluted in 2

L of ddH_2O to make 4 μM estradiol. Some of the water, with estradiol, was poured into a spray bottle to apply estradiol through an aerial spray. Plants were sprayed from above such that the leaves would not hold more water droplets. The rest of the water with estradiol was poured into the bottom of a tray to water the plants bottom-up. Both the aerial spray and bottom-up watering was done in continuous light, every other day, for one week, such that the plants were treated four times before use in continuous light, dark, light treatment, or ABA treatments.

Continuous Light Plant Material:

WS and R2-4A plants were treated with estradiol for one week. Two leaves from two different WS plants were excised with a razor blade at the base of the petiole. Epidermal peels were immediately taken from these leaves and placed on a microscope slide with *Arabidopsis* leaf buffer, 10 mM KCl, 25 mM MES, pH 6.15 (Melotto et al. 2006).

24 h Darkness Plant Material:

WS and R2-4A plants were treated with estradiol for one week. Plants were removed from continuous light and placed in a dry tray at room temperature in darkness for 24 h. After 24 h, WS and R2-4A plants were removed from the dark and two leaves from two different plants of both lines were excised under room light with a razor blade at the base of the petiole. Epidermal peels were immediately (< 5 min) taken from these leaves and placed on a microscope slide with *Arabidopsis* leaf buffer, 10 mM KCl, 25 mM MES, pH 6.15 (Melotto et al. 2006).

Light or ABA Treated Plant Material:

WS and R2-4A plants were treated with estradiol for one week. Plants were removed from continuous light and placed in a dry tray at room temperature in darkness for 24 h. After 24 h, WS and R2-4A plants were removed from the dark and placed in the light for 3 h, at 20^{o}C. After 3 h, two leaves from two different WS and R24A plants were excised and placed with the abaxial epidermis side up in a small petri plate with 3 ml *Arabidopsis* Leaf Buffer, 10 mM KCl, 25 mM MES, pH 6.15 (Melotto et al. 2006). 10 μM ABA (from a 10 mM ABA stock dissolved in 100% ethanol) or an equivalent volume of 100% ethanol (control) was added to these plates and the whole leaves were treated for a 2 h period in white light at 20^{o}C. After 2 h, epidermal peels were taken from these leaves and placed on a microscope slide.

Semi-Quantitative PCR Analysis of RNAi suppression in R2-4A line:

To confirm induction of RNAi suppression of *APY1* mRNA in mature plants treated with estradiol, total RNA was extracted (Sigma Spectrum^{TM} Plant Total RNA Kit 50 Prep) from 0.1 g mature basal leaves of WS and R2-4A lines. Reverse transcription PCR was employed to create a cDNA library and *APY1* and actin primers were used to amplify those transcripts. Primers used for *APY1* were 5'-GCAGCCGTAACTTGCAATC - 3' and 5' - CACAGCGTAATTCTTCGGACC - 3' and for actin were 5'-AACTCTCCCGCTATGTATGTCGC-3' and 5' - CCATCTCCTGCTCGTAGTCAACA - 3'. The amplified cDNA was electrophoresed on a 1% agarose gel with ethidium bromide and visualized under ultraviolet light.

Stomatal Imaging

The slides with epidermal peels were mounted on a light microscope and viewed at 200X magnification. PixeLINK Megapixel Firewire Camera and PixeLINK Capture Application were used to capture images of random stomata in the epidermal peels. In total, 60 pictures were taken of stomata, many images including more than one stoma. Stomata were randomly chosen by scrolling around the epidermal peel while looking at the digital representation (800 x 600) on the computer and avoiding the microscope eyepieces. When a stoma came into view, a picture of it was taken. The field of view in the digital representation is significantly smaller than that through the microscope eyepieces, thereby reducing bias in which stomata are chosen to be measured.

Stomatal Aperture Measurements and Analysis

After 60 pictures were taken for each WS and R2-4A treatment, the total number of open and closed stomata within each 60-picture set was determined. The percent of open stomata was calculated, and to reduce time spent taking measurements, this percent was taken out of 50. Closed stomata were represented with "0" values, and the width and length of open stomatal apertures were measured with ImageJ 1.43u. Therefore, average stomatal aperture was calculated when n=50; not all stomata in pictures were measured.

Chapter 3.2: Results

APY1 and *APY2* transcript expression is enriched in guard cells compared to mesophyll cells

Enriched guard cell protoplasts were isolated as described in Materials and Methods. Total RNA was extracted from the enriched guard cell protoplasts (high ratio of guard cells to mesophyll cells) and from whole leaves (high ratio of mesophyll cells to guard cells). Reverse transcription (RT)-PCR was used to create cDNA that was amplified with *APY1* and *APY2* primers. The amplified cDNA was electrophoresed on an agarose gel with ethidium bromide and visualized under ultraviolet light (Figure 4.5).

Gel loading of the cDNA was equivalent as determined by equal actin levels. *APY1* and *APY2* cDNA was found in greater abundance in enriched guard cell protoplasts than in whole leaves as determined by greater band intensity. These results indicate that *APY1* and *APY2* mRNA transcripts are more abundant in guard cells than in mesophyll cells, if *APY1* and *APY2* transcripts are present in mesophyll cells at all.

APY protein expression is enriched in guard cells compared to mesophyll cells

Enriched guard cell protoplasts were isolated as described in Materials and Methods. Total protein was extracted from enriched guard cell protoplasts (high ratio of guard cells to mesophyll cells) and from whole leaves (high ratio of mesophyll cells to guard cells) and was separated with SDS-PAGE. The protein was transferred from the gel to nitrocellulose and apyrase polyclonal 1^{o} antibodies were used for blotting. IRDye® 2^{o} antibodies were used for detection with the Odyssey Infrared Imaging System (Li-cor).

The Western blot revealed equal protein loading as indicated by immunodetection of α-tub. When equally loaded, APY bands from enriched guard cell protoplasts were much wider and more intense than the APY bands obtained from whole leaves (Figure 4.6). These results show that APY protein is more abundant in guard cells than in mesophyll cells, if APY is present in mesophyll cells at all.

RNAi suppression of *APY1* can be induced with estradiol in mature (3 wk old) plants of the R2-4A mutant

R2-4A mutants (*apy2* KO, estradiol-inducible RNAi suppression of *APY1*) and WS wild-type were grown on soil in continuous light until the initiation of bolting (~3 weeks). At this point, both R2-4A and WS plants were watered with 4 μM estradiol in ddH_2O every other day for 1 week (4 times in total) as described in Materials and Methods. At each watering event, plants were also treated with an aerial spray of 4 μM estradiol in ddH_2O.

After 1 week, fully expanded basal leaves were excised from both R2-4A and WS plants and total RNA was extracted. cDNA was produced using RT-PCR and was amplified with *APY1* primers. The amplified cDNA was electrophoresed on an agarose gel and visualized under ultraviolet light.

The cDNA was equally loaded in the gel as determined by near equivalent GAPDH (housekeeping gene) bands. *APY1* cDNA was more abundant in WS wild-type treated with estradiol as compared to the treated R2-4A plants as indicated by band

intensity (Figure 4.7). These results support that estradiol can induce RNAi suppression of *APY1* in mature R2-4A plants when treated every other day for one week as described.

Stomata in *apy2* mutants with *APY1* suppressed open wider after 5 h light exposure than in WS wild-type

R2-4A mutants (*apy2* KO, estradiol-inducible RNAi suppression of *APY1*) and WS wild-type were grown on soil in continuous light until the initiation of bolting. At that point, plants were treated with estradiol for 1 week as described in Materials and Methods. Treated plants were then placed in the dark for 24 h until they were transferred to light for 3 h. After 3 h, whole basal leaves were excised from the plants and placed on leaf buffer with or without ABA for 2 h in the light. Epidermal peels were taken from the leaves and stomatal aperture was measured, all as described in Materials and Methods.

After 5 h light, stomata in R2-4A peels were more open than stomata in WS plants when measuring average stomatal aperture width (Figure 4.8) or average aperture width divided by length (Figure 4.9). Average stomatal aperture width in estradiol-induced R2-4A mutants ranged from 1.7-3.3 μm while average stomatal aperture width in estradiol-treated WS ranged from 1.0-1.5 μm. Sample size n=50 was used and statistical significance was determined using Student's *t*-test. This result was repeatable in 4 of 5 experiments, and the single run that differed maintained the same trends but lacked the statistical significance (data not shown). 10 μM ABA caused closure in both WS wild-type and R2-4A plants, but after 2 h exposure to ABA, stomata in R2-4A peels remained more open than stomata in WS wild-type (Figure 4.8). This result was repeated in 3 of 4

experiments, the exception being an instance where 10 μM ABA did not cause closure in WS wild-type as expected.

Difference in stomatal aperture after 5 h light between R2-4A mutants and WS is accounted for by both a greater percent of open stomata as well as a larger average stomatal aperture width in open stomata

The percent of open stomata in R2-4A and WS aperture width comparisons was previously determined so that closed stomata were represented with "0 μm" values for average aperture width analysis. It was observed that the percent of open stomata in the estradiol-induced R2-4A mutants after 5 h light ranged from 82-93% while the percent of open stomata in WS ranged from 68-72%. These results were consistent across 4 of 5 experiments with only 68% stomata open in R2-4A peels for the non-replicate run.

Pictures used to earlier determine average aperture width were analyzed such that only the widths of open stomata were accounted for. Average stomatal width of open stomata (n=60) was significantly different between R2-4A and WS plants in 5 of 5 repeat experiments (Figure 4.10). R2-4A average stomatal width of open stomata ranged from 2.2-3.5 μm, while WS average stomatal width of open stomata ranged from 1.6-1.8 μm.

Average stomatal aperture in *apy2* mutants with *APY1* suppressed is equivalent to WS wild-type in continuous light and equivalent to or less than WS wild-type after 24 h darkness

R2-4A mutants (*apy2* KO, estradiol-inducible RNAi suppression of *APY1*) and the WS background were grown on soil in continuous light until the initiation of bolting

(~3 weeks). At that time, plants were treated with estradiol for 1 week as described in Materials and Methods. Epidermal peels were taken from WS wild-type and R2-4A plants treated with estradiol in continuous light and from plants placed in the dark for 24 h.

After 24 h dark, there was either no difference or decreased average stomatal aperture width in the R2-4A mutant compared to WS wild-type (Figure 4.11). Two of three replicates showed no difference after 24 h dark (data not shown), however Figure 4.11 shows the exception where the R2-4A mutant was more closed than WS wild-type. Stomata were mostly closed with an average stomatal aperture of approximately 0.5 μm wide. Stomata measured in plants kept in continuous light also featured no difference in average stomatal aperture width between the R2-4A mutant and WS wild-type (Figure 4.11). Stomata in continuous light were also mostly closed, as after 24 h dark, as assessed by an average stomatal aperture width of approximately 0.5 μm. For 24 h dark and continuous light stomatal aperture measurements, sample size n=50 was used and statistical significance was determined using Student's *t*-test

Chapter 4: Figures

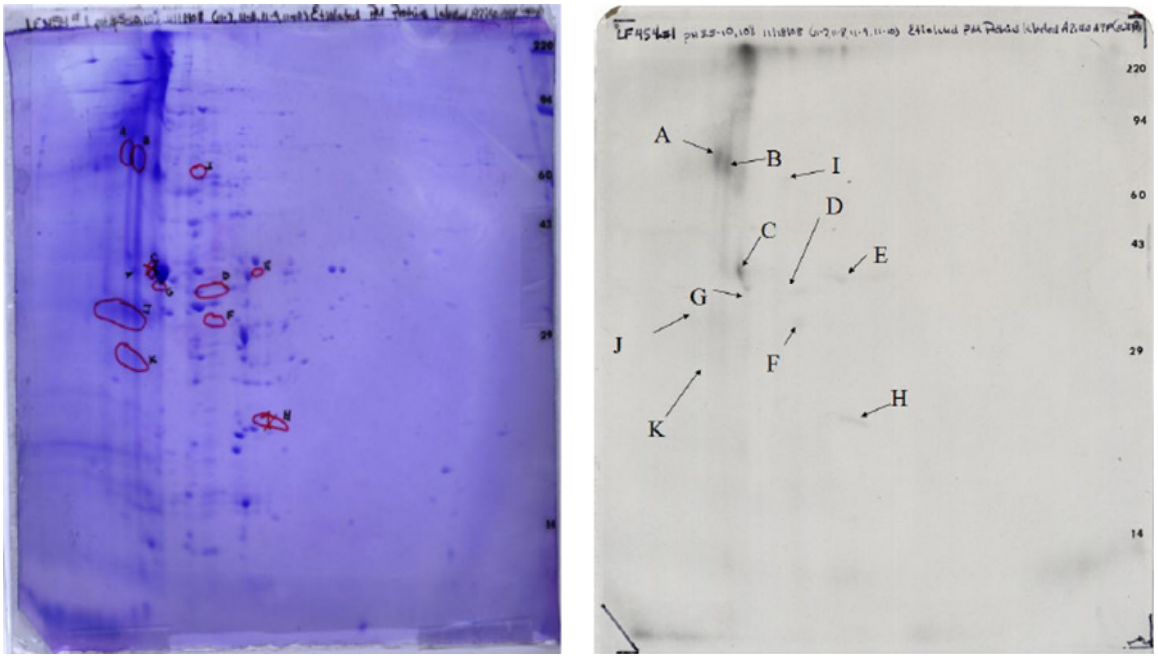

Figure 4.1: 2-D PAGE and autoradiography analysis of plasma membrane proteins obtained from etiolated seedlings and labeled with $8N_3ATP[\alpha^{32}P]$. Outside-out plasma membrane vesicles were isolated as described in Materials and Methods and proteins were labeled with $8N_3ATP[\alpha^{32}P]$. Kendrick Labs, Inc. separated the protein samples with 2D gel electrophoresis and developed an autoradiogram.

(a) Soluble Fraction

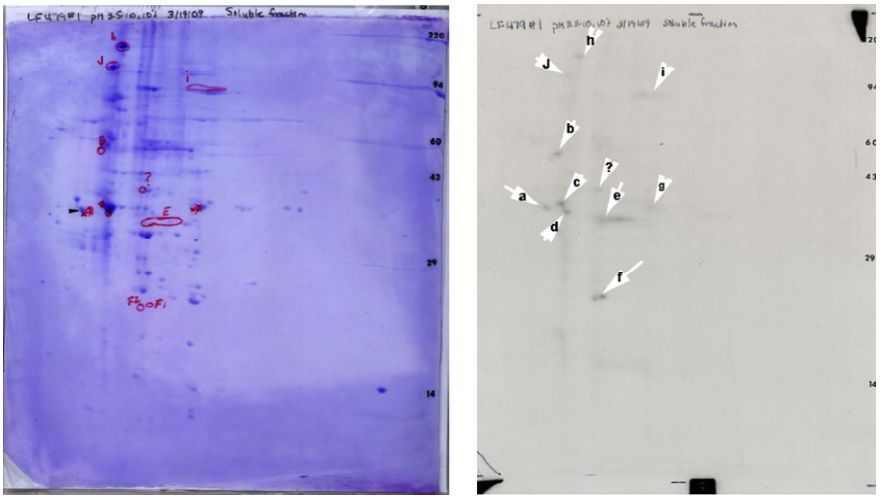

(b) Insoluble Fraction

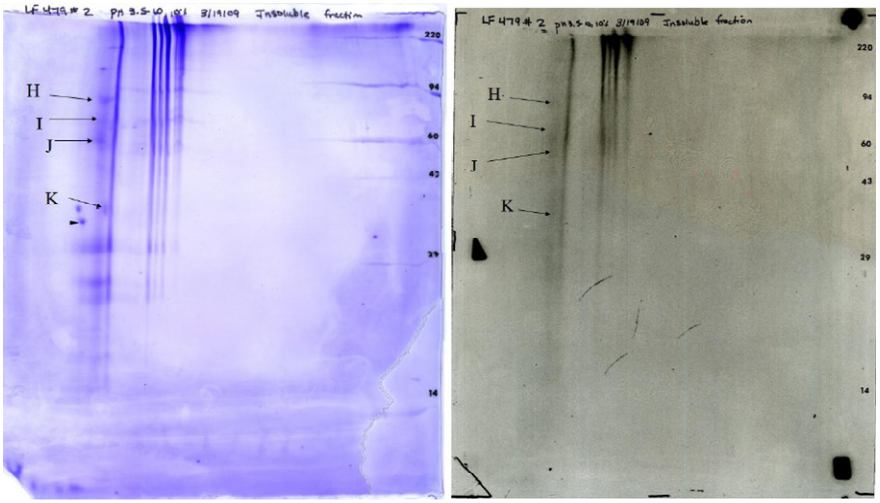

Figure 4.2: 2-D PAGE and autoradiography analysis of plasma membrane proteins labeled with 8N_3ATP[α^{32}P] and washed with sodium carbonate. Enriched outside-out plasma membrane vesicles were isolated and proteins were labeled with 8N_3ATP[α^{32}P] as described in Materials and Methods. The plasma membrane vesicles were then washed with sodium carbonate thereby producing a soluble and insoluble fraction. Kendrick Labs, Inc. separated the proteins from both samples with 2D gel electrophoresis and developed an autoradiograph for each.

Locus	Protein Description	Unique Peptides
Spot A (~X kD)		
AT4G12730	(FLA2) fasciclin-like arabinogalactan-protein 2	8
AT5G39410	Probable mitochondrial saccharopine dehydrogenase	6
AT1G22530	PATL2, PATELLIN 2, transporter	7
	6-Phosphogluconate dehydrogenase family protein	12
AT4G13930	SHM4, Serine Hydroxymethyltransferase 4	8
AtCg00490	RUBISCO, large subunit	8
AT1G20010	TUB5; tubulin beta 5 chain	7
AT4G23650	CDPK6 calcium dependent protein kinase 6	8
AT4G00710	BSK3 BR-signaling kinase 3	13
	Nucleotide Binding subunit of vacuolar ATPase	9
AT3G20410	CPK9 calmodulin-domain protein kinase	6
gi 15237465	protein kinase family protein (BSK2?)	6
AT5G62690	TUB2 encodes tubulin beta-2/beta-3 chain	8
AT4G20890	TUB9 tubulin 9	8
AT4G26110	NUCLEOSOME ASSEMLY PROTEIN 1;1	8
	beta tubulin	7
	S-adenosyl-L-homocysteine hydrolase	5
	S-adenosyl-L-homocysteine hydrolase	7
AT1G20440	COR47 Cold-regulated 47	2
AT5G41260	protein kinase family protein	5
AT5G58090	glycosyl hydrolase family 17 protein	5
AT1G44170	ALDH3H1 ALDEHYDE DEHYDROGENASE 4	1
AT5G44130	FLA13, Fasciclin-like arabinogalactin protein 13	1
AT1G72150	PATL1 PATELLIN 1	2
AT1G49740	phospholipase C, map3k-like protein kinase	2
AT4G35230	BSK1, BR-SIGNALING KINASE1	3

Locus	Protein Description	kDa
Spot I		
AT4G14030	selenium-binding protein, putative protein kinase	54.057
Spot E		
AT1G13440	GAPC-2	36.913
Spot D		
AT5G65020	ANNAT2, ANNEXIN ARABIDOPSIS 2	36.266
Spot G		
AT2G18020	60S ribosomal protein L8-1	27.859

Figure 4.3: LC/MS-MS results from $8N_3ATP[\alpha^{32}P]$-labeled enriched outside-out plasma membrane vesicle proteins isolated from etiolated seedlings. Enriched outside-out plasma membrane vesicles were isolated and labeled with $8N_3ATP[\alpha^{32}P]$ as described in Materials and Methods. The protein was separated on a 2-D gel, an autoradiogram was produced, and specific spots (A, I, E, D, and G) were cut out and sequenced with LC/MS-MS.

(a) Soluble Fraction

Locus	Protein Description	Unique Peptides
Spot I (soluble)		
At5g17920	5-methyltetrahydropteroyltriglutamatehomocysteine methyltransferase	29
AT4G12420	SKU5 Putative monocopper oxidase	14
Spot B (soluble)		
AT1G20010	TUB5	14
Spot ? (soluble)		
At1g79550	Phosphoglycerate Kinase	17
At1g56190	phosphoglycerate kinase	7
Spot E (soluble)		
AT5G65020	ANNAT2, ANNEXIN ARABIDOPSIS 2	21
AT1G20440	COR47 Cold-regulated 47	2
AT5G41260	protein kinase family protein	5
AT5G58090	glycosyl hydrolase family 17 protein	5
AT1G44170	ALDH3H1 ALDEHYDE DEHYDROGENASE 4	1
AT5G44130	FLA13, Fasciclin-like arabinogalactin protein 13	1
AT1G72150	PATL1 PATELLIN 1	2
AT1G49740	phospholipase C, map3k-like protein kinase	2
AT4G35230	BSK1, BR-SIGNALING KINASE1	3

(b) Insoluble Fraction

Locus	Protein Description	Unique Peptides
Spot H (insoluble)		
At5g02500	HEAT SHOCK COGNATE PROTEIN 70	23
AT5G42020	LUMINAL BINDING PROTEIN	16
AT1G78900	VACUOLAR ATP SYNTHASE SUBUNIT A	13
Spot I (insoluble)		
At2g20990	SYNAPTOTAGMIN A	20
Spot J (insoluble)		
	Keratin 10 Human	20
AT2G29550	TUB7, Tubulin beta-7 chain	15

Figure 4.4: LC/MS-MS results from $8N_3ATP[\alpha^{32}P]$-labeled enriched outside-out plasma membrane proteins washed with sodium carbonate. Enriched outside-out plasma membrane vesicles were isolated, labeled with $8N_3ATP[\alpha^{32}P]$, and washed with sodium carbonate to produce a soluble (peripheral) and insoluble (insoluble) protein fraction as described in Materials and Methods. Both fractions were separately run on 2-D gels, autoradiograms were produced, and specific spots (insoluble: H, I, J; soluble: B, E, I, ?) were cut out and sequenced with LC/MS-MS.

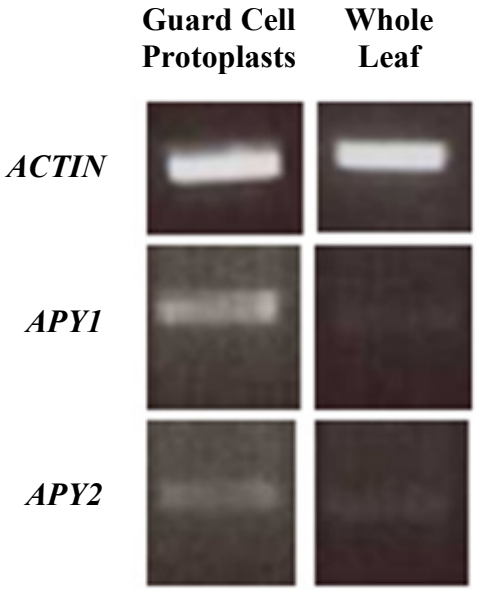

Figure 4.5: *APY1* and *APY2* transcripts are expressed in guard cell protoplasts. Total RNA was extracted from enriched guard cell protoplasts (isolated as described in Materials and Methods) and whole leaves. cDNA was produced with reverse transcription, amplified with *APY1* and *APY2* primers, and separated with gel electrophoresis to determine relative abundance of *APY1* and *APY2*..

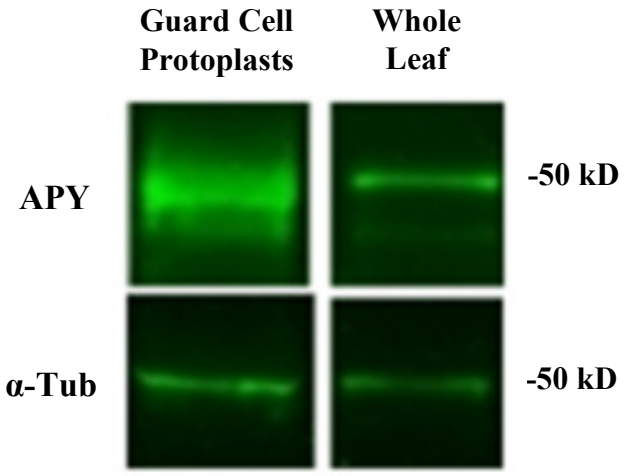

Figure 4.6: Western blot analysis shows APY protein expression in guard cells. Total protein was extracted from enriched guard cell protoplasts (GCP) obtained as described in the Materials & Methods and from whole leaves. Proteins were separated with SDS-PAGE, transferred to nitrocellulose, and detected with either polyclonal anti-apyrase 1^{o} antibodies or monoclonal anti-α-Tubulin Ab (Rockland) and anti-guinea pig 2^{o} antibodies or anti-mouse 2^{o} antibodies, respectively.

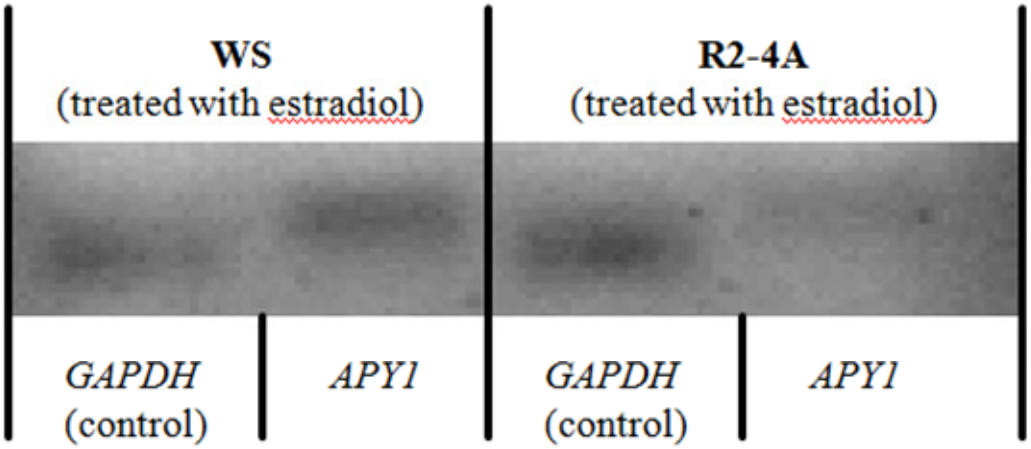

Figure 4.7: Estradiol can induce RNAi suppression of *APY1* in mature leaves of the R2-4A mutant. WS and R2-4A 3-week old plants were treated with 4 μM estradiol as described in Materials and Methods. Total RNA was extracted from mature basal leaves and relative *APY1* levels were determined with reverse transcription (RT)-PCR.

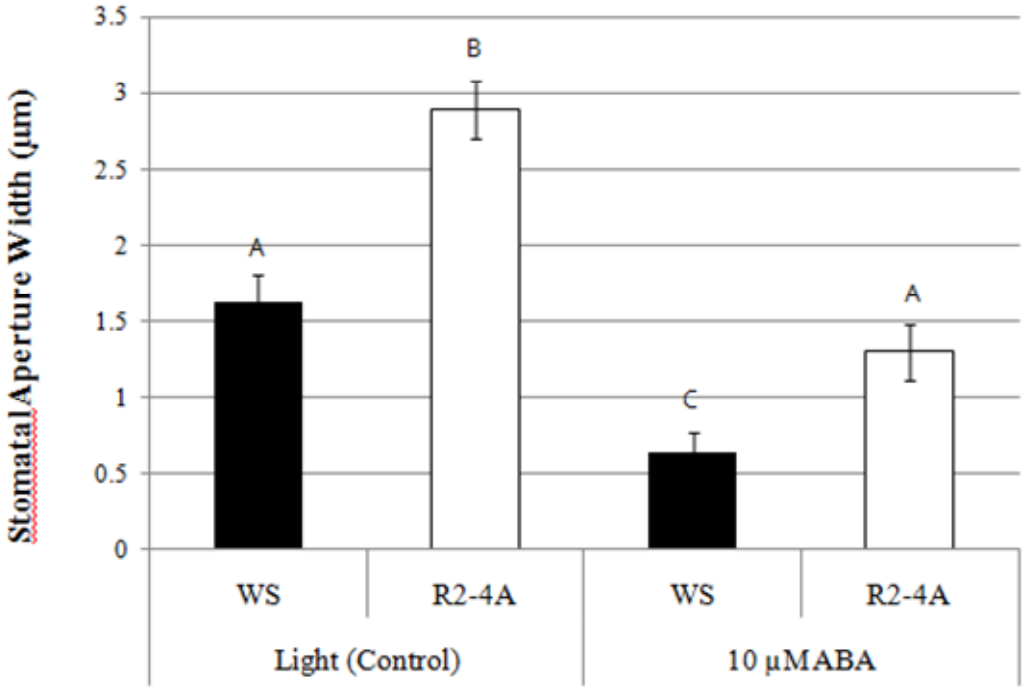

Figure 4.8: RNAi suppression of *APY1* in an *apy2* single knockout results in wider average stomatal aperture width than WS wild-type in response to treatment with 5 h light. 3-4 week old plants grown in continuous light were placed in the dark for 24 h. The plants were then transferred to the light for 3 h, whole leaves were excised, and the leaves were placed in the light for 2 h on buffer with the treatment (10 µM ABA or control) as described in Materials and Methods. Epidermal peels were obtained from the leaves and stomatal aperture measurements were recorded.

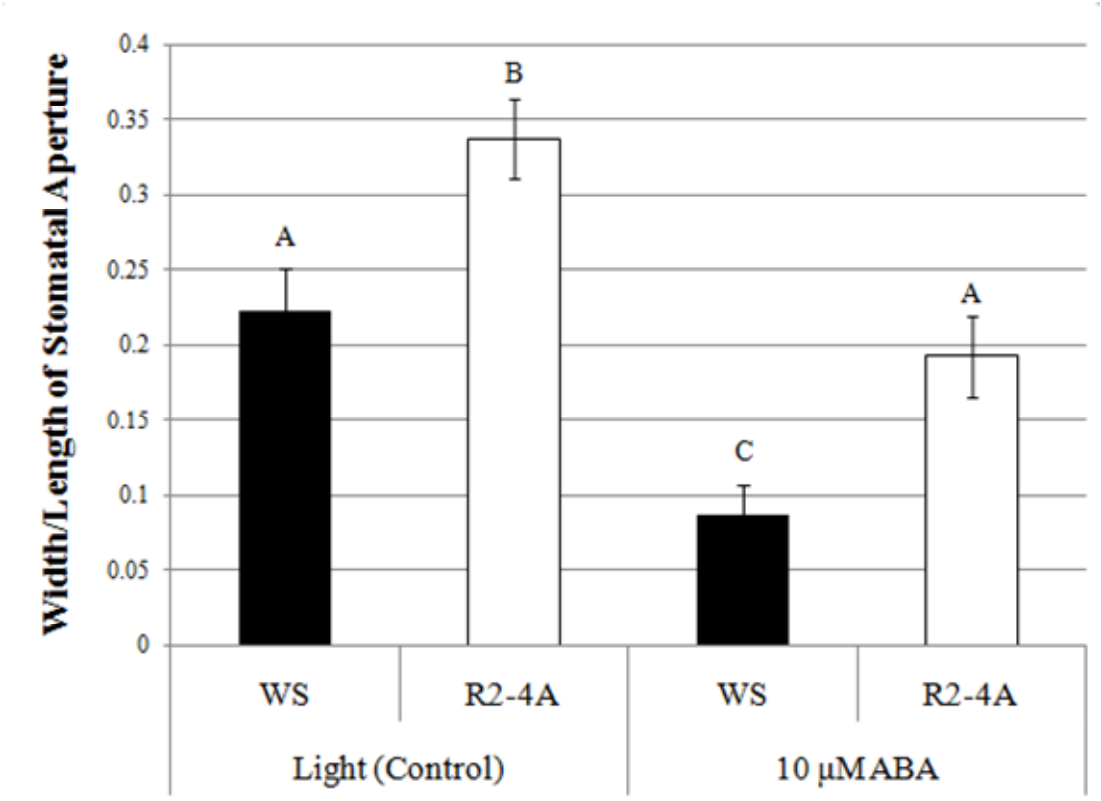

Figure 4.9: RNAi suppression of *APY1* in an *apy2* single knockout results in increased width divided by length values than WS wild-type in response to treatment with 5 h light. 3-4 week old plants grown in continuous light were placed in the dark for 24 h. The plants were then transferred to the light for 3 h, whole leaves were excised, and the leaves were placed in the light for 2 h on buffer with the treatment (10 µM ABA or control) as described in Materials and Methods. Epidermal peels were obtained from the leaves and stomatal aperture measurements were recorded. This figure represents an alternative data analysis where width/length is recorded instead of width alone.

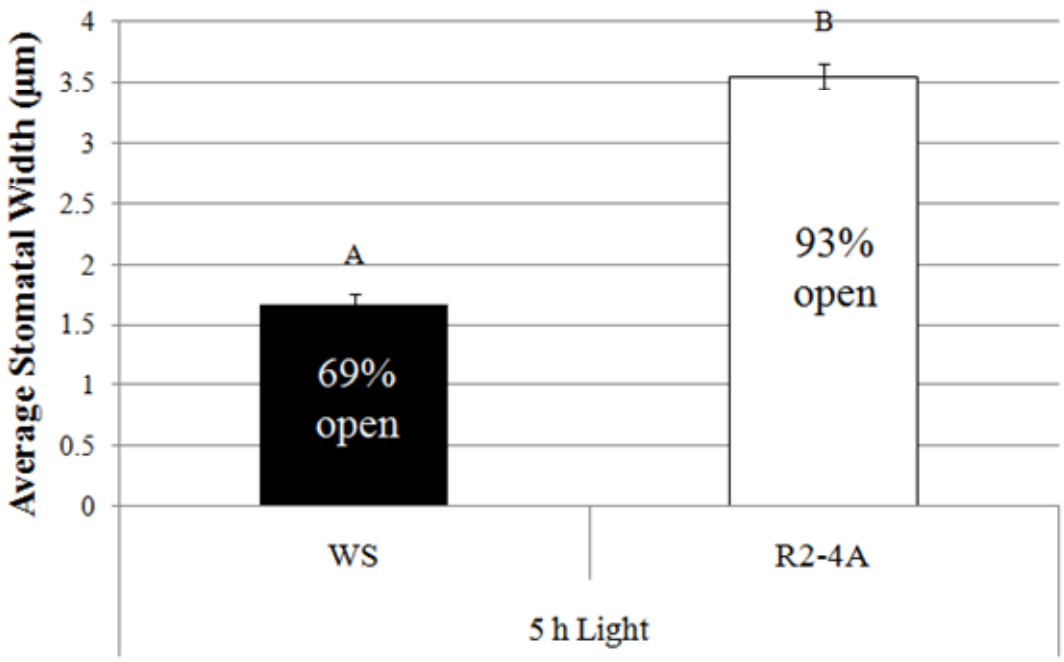

Figure 4.10: RNAi suppression of *APY1* in an *apy2* single knockout results in increased average stomatal aperture width amongst open stomata as compared to WS wild-type in response to treatment with 5 h light. Stomatal aperture pictures previously collected and analyzed (Figure 4.8) were measured in an alternate manner such that only open stomata in WS and R2-4A plants were taken into account. The percentage in each column describes the percent of open stomata (versus closed) in each sample. The statistical difference in stomatal aperture width of open stomata was consistent across 5 of 5 separate experiments.

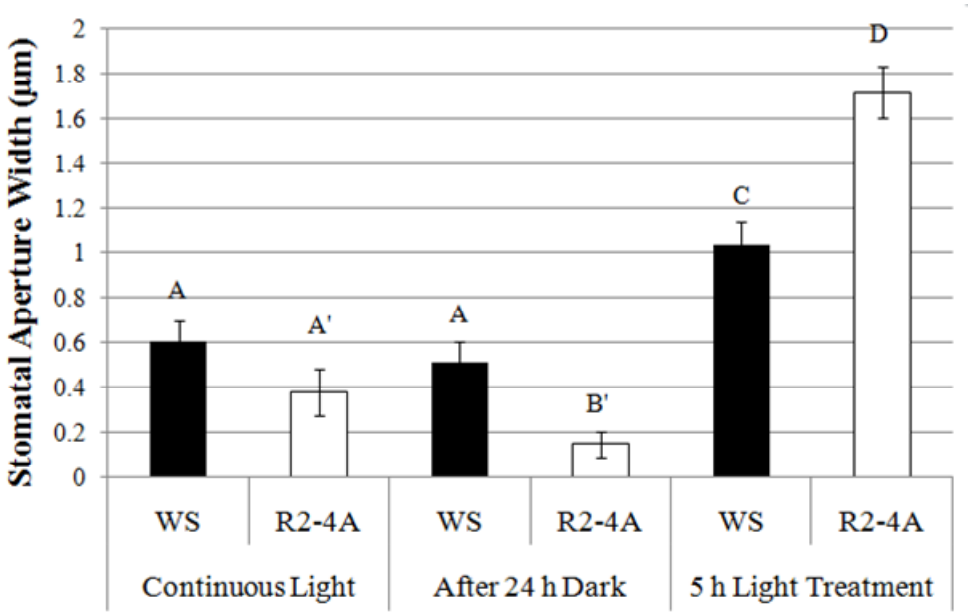

Figure 4.11: Average stomatal aperture in *apy2* mutants with *APY1* suppressed is equivalent to WS wild-type in continuous light and equivalent to or less than WS wild-type after 24 h darkness. Epidermal peels from 3-4 week old plants grown in continuous light were obtained and pictures of stomata were taken. The plants were then placed in the dark for 24 h after which epidermal peels were obtained again and pictures were taken. The plants were then transferred to the light for 3 h, whole leaves were excised, and the leaves were placed in the light for 2 h on buffer as described in Materials and Methods. Epidermal peels were also obtained from these leaves and pictures were taken. From pictures, average stomatal width was measured as described in Materials and Methods. The statistically significant difference between R2-4A and WS wild-type after 24 h darkness was only observed in 1 of 3 replicate experiments, but this figure was selected because it was the sole experiment that examined stomata in continuous light, after 24 h darkness, and after 5 h light simultaneously.

Chapter 5: Discussion

Radiolabeling approach with $8N_3ATP[\alpha^{32}P]$ and enriched outside-out plasma membrane vesicles to the identification of a plant purinoceptor-like receptor

Enriched outside-out plasma membrane vesicles were isolated from etiolated seedlings and labeled with $8N_3ATP[\alpha^{32}P]$ as described in Materials and Methods. The plasma membrane proteins were separated on a 2-D gel and identified by Coomassie staining and autoradiography. The Coomassie stained gel and autoradiography were overlaid to identify common spots between them to be cut out and sequenced.

The use of $8N_3ATP[\alpha^{32}P]$ to label unknown purinoceptors in enriched outside-out plasma membrane vesicles was previously done in light grown tissues (Butterfield 2007). The analog $8N_3ATP[\alpha^{32}P]$ was chosen because the azido group allows for covalent linkage to the bound protein under UV radiation and because the ^{32}P isotope exists on the α-phosphate group. Earlier experiments by Butterfield (2007) were done with an ATP analog where ^{32}P existed on the γ-phosphate, and it was determined that labeled proteins may be those that accepted a cleaved γ-phosphate. Therefore, the use of $8N_3ATP[\alpha^{32}P]$ should limit radio-labeled proteins to those that bind ATP, not a cleaved terminal phosphate, as a purinoreceptor would be expected to bind.

In contrast to the experiments by Butterfield (2007), the use of etiolated, or dark grown seedlings is reported here. As discussed in Chapter 1 (Introduction), ATP is secreted from growing tissues in *Arabidopsis* where strongly expressed enzymes (APY1 and APY2) are thought to regulate and reduce the concentration of eATP to allow faster growth. Therefore, it was hypothesized that a purinoceptor-like receptor would be heavily

expressed in growing tissues where eATP plays a significant role. Growth in dark conditions results in etiolated seedlings featuring white coloring and an apical hook, but also elongated hypocotyls. Seedlings were grown in the dark for 3.5 days to examine the plasma membrane proteins at a time when hypocotyls would experience an accelerated rate of growth and possible increased expression of a purinoceptor-like receptor.

Several spots were identified on the autoradiogram and labeled A-H (Figure 4.1). The presence of several spots on the autoradiogram suggests that $8N_3ATP[\alpha^{32}P]$ bound to numerous proteins. As it is inefficient and costly to sequence all spots on the autoradiogram, it was necessary to select candidate spots that were most likely to contain the protein of interest. These selections were not random and were based on recommendations from Kendrick Labs Inc. regarding the size of the autoradiogram spot and the presence of Coomassie staining at a matching spot in the overlay. Furthermore, spots falling between 40-60 kD were of particular interest based on the typical size of P2X receptors in animals. While the spots were not arbitrarily selected, those not analyzed remain unknown and could potentially represent a plant purinoceptor-like receptor.

Here, spots A, D, E, G, and I were sequenced (Figure 4.3). Detailed results from spot A are shown, and only the most abundant protein is listed for the rest. Spot A revealed peptides from 26 different proteins making it clear that many proteins can be sequenced from each spot. Despite plasma membrane protein enrichment and 2-D gel separation, the proteins were not separated enough to resolve which protein was bound to

the isotope. For this reason, it is difficult to narrow down the sequenced proteins to a putative purinoceptor-like receptor.

Some sequenced proteins have been previously identified as plasma membrane proteins in similar plasma membrane isolations. These include fasciclin arabinogalactan-protein (FLA2:At4g12730) and calmodulin-domain protein kinase (CPK9:At3g20410) (Alexandersson et al. 2004), but other proteins including rubisco large subunit (AtCg00490) and 60S ribosomal protein L8-1 (At2g18020) are known cytosolic contaminants. Therefore, while the protein sample consisted of plasma membrane proteins, the impurity makes it more difficult to identify putative purinoceptor-like receptors from poorly described proteins with an unknown subcellular locale.

Though part of the idea of using etiolated seedlings was to generate plasma membrane enriched with a purinoceptor-like receptor, there is no reason to believe light grown tissue is void of purinoceptor-like receptors. As a result, the proteins sequenced here (Figure 4.3) were compared with the proteins identified in similar experiments by Butterfield (2007) using both $8N_3ATP[\gamma^{32}P]$ and $8N_3ATP[\alpha^{32}P]$ to label enriched outside-out plasma membrane vesicles. A number of overlapping proteins were identified including phospholipase C (PLC2) and annexin 2 (AnnAt2). Fasciclin-like arabinogalactan (FLA) and patellin (PATL) family members also overlapped.

However, while PATL family members and PLC2 are membrane-associated proteins, they are known to act on the cytosolic-side of the membrane. PATL1, for instance, is a PI-binding protein important in membrane trafficking and is recruited at the cell plate (Peterman et al. 2004). PLC2, and other phospholipases, bind to PIPs at the

cytosolic surface of the plasma membrane (Otterhag et al. 2001) and should also not bind $8N_3ATP[\gamma^{32}P]$ when pure outside-out plasma membrane vesicles are labeled. If PLC2 and PATL are directly labeled, this suggests that the outside-out plasma membrane isolation was contaminated with inside-out vesicles. However it is likely, considering the 26 different proteins sequenced at spot A alone, that PLC2 and PATL proteins run at the same spot on a 2-D gel as another protein that consistently bound $8N_3ATP[\gamma^{32}P]$ in sufficient abundance to produce autoradiogram spots.

The reoccurrence of the same or similar proteins in labeled spots may or not may not be exciting. It is possible that these proteins reoccur (amongst other proteins that have been sequenced in one experiment and not in another) because they consistently bind to $8N_3ATP[\alpha^{32}P]$. Alternatively, these proteins may merely be abundant and run to the same spot on the 2-D gel as a less-plentiful radiolabeled protein.

It was concluded that to perform follow-up studies on one or more purinoceptor-like receptor candidates, it was necessary to develop a new method to reduce the number of proteins sequenced from a spot on the 2-D gel.

In order to address both the problem of sequencing too many proteins per spot and to ask whether the ATP-binding proteins are integral or peripheral membrane proteins, the same approach was used as previously described with modifications. Plant material was grown in the light in a liquid medium so as to generate more starting material and ultimately a greater outside-out plasma membrane vesicle yield. After outside-out plasma membrane vesicles were isolated and labeled with $8N_3ATP[\alpha^{32}P]$, the membrane was washed with sodium carbonate to solubilize peripheral membrane proteins. Therefore, a

soluble protein fraction containing peripheral membrane proteins and a separate insoluble protein fraction with integral membrane proteins was created.

Despite starting with more plant material, this isolation yielded half the total protein obtained in the etiolated run. Still, the soluble fraction produced a 2-D gel with numerous Coomassie stained spots, indicating that protein yield was sufficient (Figure 4.2). Relative to the soluble fraction, the insoluble protein fraction revealed few Coomassie-stained spots when separated on a 2-D gel (Figure 4.2). Similarly, the autoradiogram developed from the soluble protein fraction featured 8 spots (labeled A-G + ?) while the insoluble fraction autoradiogram only had 4 spots (labeled H-K). The difference in labeling may either be due to less ATP-binding proteins in the insoluble fraction, or due to a lesser abundance of proteins in the insoluble fraction as supported by the relatively barren Coomassie staining.

As with the previously described experiment from etiolated tissue, select spots were chosen to be sequenced. From the soluble fraction 2-D gel, spots B, E, I, and "?" were cut out and sequenced (Figure 4.4). Previous to the experiment, it was hypothesized that separation of peripheral and integral membrane proteins would reduce the number of proteins sequenced in a particular spot, thereby making it easier to resolve what proteins were bound to $8N_3ATP[\gamma^{32}P]$. Comparing spot A results from the etiolated run (Figure 4.3) with the spot E results from the soluble fraction (Figure 4.4), this approach, using a sodium carbonate wash, did not necessarily resolve the issue. While the number of unique proteins was certainly less, a number of proteins were still sequenced per spot. Furthermore, the proteins that did not appear in spot E and did appear in the comparable

spot A were not identified in the insoluble fraction suggesting their absence was a matter of protein abundance or their consistency in binding ATP, not necessarily a result of the sodium carbonate wash.

If the plasma membrane isolation was impure and contained cytosolic contaminants, it would be expected that they would be most abundant in the soluble fraction. Still, many of the proteins sequenced have been previously identified in plasma membrane protein isolations including ATMS1 (At5g17920), SKU5 (At4g12420), and ASNAP (At1g56190) (Alexandersson et al. 2004) and no known contaminants were identified. This suggests the plasma membrane isolation was pure in regards to contaminating cellular components.

From the insoluble fraction 2-D gel, two of three spots were cut out and sequenced: H, I, and J. These spots did contain considerably less proteins per spot, but this may be the result of less loaded protein. Since there were less spots to choose to sequence from, spots were sequenced from molecular weight/isoelectric points not chosen before. As a result, proteins were sequenced that had not been identified in earlier experiments. The known roles of the insoluble fraction proteins does not make them strong candidates for purinoceptor-like receptors and further focus in this discussion is aimed at soluble fraction proteins.

Many proteins identified in the soluble fraction were also identified in previous experiments including the one earlier described in this thesis and those performed by Butterfield (2007). Overlapping proteins between the soluble fraction and the etiolated experiment earlier described include cold-regulated 47 (COR47), brassinosteroid

signaling kinase (BSK1), annexin 2 (AnnAt2), phospholipase C (PLC2), fasciclin-like arabinogalactic protein 13 (FLA13), and aldehyde dehydrogenase 4 (ALDH3H1). The large number of overlapping proteins identified in one spot, as these were all in spot E of the soluble fraction, again suggests that the sodium carbonate wash is not an effective means of gaining better resolution since the proteins identified in commonly labeled spots are mostly soluble proteins.

Overlapping proteins between the experiments described in this thesis and those done by Butterfield (2007) include patellin 1 (PATL1), phospholipase C (PLC2), and annexin 2 (AnnAt2). Though the member of the family varied per experiment, FLA proteins were also identified in each experiment. As previously explained, PATL1 and PLC2 associate with the plasma membrane, but on the cytosolic side. Therefore, the outside-out plasma membrane vesicles were either impure and contained inside-out vesicles, or PATL1 and PLC2 are not directly labeled and instead run to a similar spot on the 2-D gel as a commonly labeled protein.

Contrastingly, FLA proteins and AnnAt2 remain possible purinoceptor-like receptors based on their identification at $8N_3ATP[\gamma^{32}P]$-labeled spots and known subcellular locale. At least 21 different FLA proteins in *Arabidopsis* constitute a glycosylated protein family in contact with the extracellular matrix, where they play a role in cell adhesion (Johnson et al. 2003). Annexins, as a family, are known to localize to plasma membranes in plants (Clark et al. 1992) and be released to the extracellular space in animals (Ma et al. 1994). As it remains unknown whether or not AnnAt2 has an extracellular facing domain, it is another possible candidate based on this radiolabeling

approach. While only proteins that were identified in multiple experiments were discussed here, it is possible that a plant purinoceptor-like receptor is not strongly expressed and may not have been identified in all, if any, of the experiments described.

It was concluded that 2-D PAGE is unable to sufficiently separate plasma membrane proteins labeled with $8N_3ATP[\gamma^{32}P]$ to resolve which proteins were bound to the isotope. Sodium carbonate was used to release peripheral membrane proteins from integral membrane proteins, but still too many proteins were sequenced in each spot. This indicated that sodium carbonate separation did not help resolution in the 2-D gel. It was also observed that the majority of autoradiography spots were found in the soluble protein fraction, where many proteins were identified that had been earlier sequenced in the etiolated experiment. This suggests that most of the $8N_3ATP[\gamma^{32}P]$ binding proteins act as peripheral membrane proteins.

Apyrase expression studies in guard cells

Enriched guard cell protoplasts were isolated from 3-4 week old *Arabidopsis* as described in Materials and Methods. Total RNA was extracted from enriched guard cell protoplasts and whole leaves. Reverse transcription PCR was used to create cDNA that was amplified with *APY1* and *APY2* specific primers and analyzed with semi-quantitative PCR.

Prior to the experiment, preliminary *APY1* and *APY2* promoter:GUS expression from Dr. Iris Steinebrunner (unpublished) suggested *APY1* and *APY2* were expressed in guard cells and not mesophyll cells. Therefore, as the enriched guard cell protoplast samples exhibit a high ratio of guard cells to mesophyll cells (Pandey et al. 2002), it was

hypothesized that they would have greater *APY1* and *APY2* transcript expression than whole leaves where the guard cell to mesophyll cell ratio is significantly smaller.

Indeed, semi-quantitative PCR analysis shows that both *APY1* and *APY2* transcript expression is stronger in enriched guard cell protoplasts than whole leaves (Figure 4.5). Therefore, *APY1* and *APY2* mRNA is expressed in guard cells. Though *APY1* and *APY2* mRNA is found in guard cells, the possibility of post-transcriptional control made it essential to also confirm APY protein expression in guard cells.

Enriched guard cell protoplasts were isolated from 3-4 week old *Arabidopsis* as described in Materials and Methods. Total protein was extracted from enriched guard cell protoplasts and whole leaves. Protein was separated with SDS-PAGE, transferred to nitrocellulose, and immunoblotted with apyrase antibodies (non-specific amongst APY1 and APY2).

As a result of *APY1* and *APY2* mRNA expression results, it was hypothesized that APY1 and APY2 protein are expressed in guard cells. Consistent with semi-quantitative PCR, apyrase protein is more strongly expressed in enriched guard cell protoplasts than in whole leaves (Figure 4.6). APY protein in guard cells and *APY1* and *APY2* mRNA in guard cells together suggest that both APY1 and APY2 are expressed in guard cells of mature basal leaves.

Less intense bands for APY1 and APY2 in whole leaves for both semi-quantitative PCR and Western blot data can be explained by the presence of guard cells in whole leaves. Still, it could not be determined if apyrase was also expressed in mesophyll cells but to a lesser extent. Regardless, increased or sole expression of APY1

and APY2 in guard cells of mature leaves, relative to mesophyll cells making up the majority of leaf tissue, suggests a unique role for apyrases in guard cell functioning. As discussed in Chapter 1 (Introduction), APY1 and APY2 are thought to act as ectoapyrases where they regulate the novel plant signaling agent eATP. Therefore, the expression of apyrases in guard cells also supports a role for eATP in guard cell signaling. Considering the primary function of guard cells is to regulate the opening or closure of stomata, the unique expression of APY1 and APY2 suggests a role for them and eATP in stomatal regulation.

Of two enriched guard cell protoplast isolations described by Pandey et al. (2002), an overnight method was selected that yields double the guard cell protoplasts of the same-day protocol also described. However, it was stated that longer exposure to the enzyme solution using the overnight method could more heavily impact guard cell protoplast physiology (Pandey et al. 2002). In defense of the overnight method, patch clamping studies and ABA-driven ion currents are comparable between short (Wang et al. 2001, Pandey et al. 2002) and long (Pei et al. 1997) protoplasting protocols as mentioned by Pandey et al. (2002).

Though guard cell protoplasts demonstrate physiological responses, including to the stress hormone ABA, it was of concern that APY expression comparison between enriched guard cell protoplasts and whole leaves was not a properly controlled experiment. As the guard cell protoplasts undergo stresses including cell wall digestion and possibly osmotic stress, it was considered that the act of protoplasting may upregulate apyrases and therefore stronger expression would be observed than in whole

leaf tissue (where protoplasting was not done). This remains a concern and can be answered by comparing apyrase levels in mesophyll cell protoplasts (Yoo et al. 2007) and guard cell protoplasts (Pandey et al. 2002).

Genetic studies for the role of APY1 and APY2 in stomatal regulation

Since APY1 and APY2 are expressed in guard cells, it followed that *apy1* and *apy2* knockouts should be evaluated for altered stomatal responses to the well-characterized stimuli light and ABA. As discussed in Chapter 1: Introduction, *apy1* and *apy2* single knockouts exhibit minor phenotypes. As APY1 and APY2 act mostly redundantly, single knockout stomatal phenotypes were not evaluated in this thesis. Instead, R2-4A mutants were selected that have *apy2* knocked out and *APY1* suppressed with RNAi under the inducer estradiol (Wu et al. 2007).

When treated with estradiol, thereby suppressing *APY1*, R2-4A mutants feature a variety of phenotypes including significantly shorter root and hypocotyl lengths and smaller leaves than the WS wild-type (Wu et al. 2007). In order to assay stomatal responses to light or ABA, it is necessary to obtain an epidermal peel from leaves. Due to the small size of induced R2-4A leaves, peels could not be obtained. Furthermore, it could be argued that changes in stomatal responses observed in induced R2-4A plants was a secondary effect of other severe phenotypes observed, not due to the lack of APY1 and APY2 in stomata. To examine the induced R2-4A phenotype in stomata, plants were treated with estradiol after development of the mature basal leaves. Late RNAi induction allowed the basal leaves to fully expand before used in experiments.

Since R2-4A plants were not treated with estradiol until they were done growing, obvious phenotypes such as those observed in R2-4A mutants planted with estradiol were not observed. It could be reasoned that the thicker plant tissue and cuticle would inhibit or reduce uptake of estradiol into mature plant cells. Therefore, it was necessary to confirm *APY1* RNAi suppression after treatment with estradiol as described in Materials and Methods. Semi-quantitative PCR shows suppression of *APY1* transcript in induced R2-4A leaves compared to the WS wild-type (Figure 4.7). However, an attempt to quantify *APY1* suppression with qtPCR was not successful so it remains unknown if the suppression induced in mature plants is equivalent to the suppression of *APY1* in seedlings grown on estradiol (Wu et al. 2007).

Preliminary data from undergraduate students working under the direction of Dr. Greg Clark (unpublished) demonstrate the ability of high concentrations (175+ μM) of applied non-hydrolyzable ATP and ADP analogs (ATPγS and ADPβS) to induce stomatal closure in light, while low concentrations (5-15 μM) induce stomatal opening in the dark. Furthermore, Dr. Greg Clark's students have shown that chemical inhibition of APY1 and APY2 induce stomatal closure in the light with both antibodies and inhibitors. As discussed in Chapter 1: Introduction, evidence suggests APY1 and APY2 act as ectoapyrases where they reduce [eATP]. Therefore, it was hypothesized that the presence of APY1 and APY2 in guard cells reduces [eATP] and promotes stomatal opening.

R2-4A mutants and the WS wild-type were grown in continuous light and treated with estradiol. Plants were placed in the dark for 24 h to close stomata and then leaves were exposed to light for a total of 5 h as described in Materials and Methods. Average

stomatal aperture width was determined for R2-4A and WS leaves exposed to 5 h light (control) and for those treated with 10 μM ABA for 2 h of the total 5 h in the light (Figure 4.8).

As reported above (Fig 4.8), stomatal aperture width of the apyrase suppressed R2-4A mutant exceeded the width of WS wild-type after 5 h light. This result was observed in 4 of 5 experiments, and the sole experiment that did not repeat the results followed the same trend without statistical significance. It remains unclear how the results of genetic suppression of APY1 and APY2 on stomata fits with the model of eATP regulation because the opposite effect on stomata is observed in response to their chemical suppression (Clark et al. unpublished). Earlier studies show that APY1 and APY2 are expressed in other expanding cells where high applied [eATP], apyrase inhibitors, and RNAi suppression of apyrase expression inhibit growth (Wu et al. 2007, Reichler et al. 2009, Clark et al. 2010a). Contrastingly, the results presented here show that late-induced RNAi suppression of apyrase expression enhances stomatal opening in white light. Still, replicate experiments suggest the opening of R2-4A stomata is not the result of error, and the differing effects between chemical and genetic inhibition of apyrase must be resolved.

Many explanations for the results described here have been considered including that "low" concentrations (5-15 μM) of applied ATPγS that induce opening are similar to the higher levels of eATP expected in the apyrase suppressed R2-4A mutant. This reasoning assumes that concentrations of apyrase inhibitors and antibodies that cause stomatal closure also inhibit apyrase activity more than the RNAi suppression of apyrase

does, thereby increasing the [eATP] to sufficiently high levels that inhibit stomatal opening. To test this hypothesis, it would be necessary to determine if the [eATP] in the ECM of guard cells is different when APY1 and APY2 are chemically suppressed than occurs in the induced R2-4A mutant.

Stomatal closure in response to ABA was also observed in WS wild-type and the R2-4A mutant (Figure 4.8). 10 μM ABA exposed to whole leaves for 2 h in the light caused closure in both WS wild-type and R2-4A mutant, however the average stomatal widths after 2 h ABA treatment was not equal between them. As after 5 h light, R2-4A was more open after ABA than WS. However, it is notable that ABA generally caused the same percent closure in both R2-4A and WS. Therefore, it may be that ABA acts equally on R2-4A and WS and that the difference observed between them is the result of R2-4A being more open before treatment with ABA. It is also possible that after 2 h ABA treatment, stomata have fully responded to ABA and are no longer undergoing closure. In this case, it may be that R2-4A resists stomatal closure as signaled by ABA. This could be better clarified by performing the same experiment with longer leaf exposure to ABA.

There are multiple ways, all commonly found in plant literature, by which stomatal aperture is determined. These methods include the measurement of stomatal aperture width, the measurement of aperture width divided by aperture length, and by measuring the rate of transpiration. It is possible that while the WS wild-type had a smaller average aperture width, the stomata measured may have been smaller as a whole and also had a smaller average aperture length. In this case, the width would suggest the

stomata were more closed, whereas the stomata could be small and actually as open as possible. Here, the same pictures measured to determine stomatal aperture width were also used to determine aperture width divided by length (Figure 4.9). These results were consistent with those collected for average aperture width. Across five experiments, slight differences existed in the response of R2-4A to ABA, but no consistent differences were observed.

As part of determining average stomatal aperture width and width divided by length, closed stomata are represented with zero values. Therefore, the difference in stomatal aperture observed after 5 h light (Figure 4.8, Figure 4.9) could be the result of a larger percentage of open stomata, stomata that are more open, or both. The percent of open stomata was determined from the same pictures used in aperture width measurements and average aperture width of open stomata was determined (Figure 4.10). R2-4A stomata were 93% open compared to 69% open in WS wild-type, but also the average aperture width of open stomata was significantly greater in R2-4A mutant. As R2-4A mutant stomata were more open in both regards, the function of APY1 and APY2 in stomatal opening could not be narrowed down.

Average stomatal aperture size was greater in R2-4A mutants than WS wild-type after 5 h light, but this result could be due to stomata that resist closure in the dark. Stomatal aperture width was determined for induced R2-4A mutants and WS wild-type both in continuous light and immediately after 24 h darkness (Figure 4.11). The aperture width for stomata in continuous light and after 24 h dark was statistically equal, except for R2-4A stomata after 24 h darkness where more closure than WS wild-type was

observed. This exception was not repeated in 2 of 3 experiments with continuous light and 24 h darkness suggesting that WS and R2-4A stomata are equally closed in continuous light and after 24 h darkness. The stomatal aperture in leaves of both WS wild-type and R2-4A mutant stomata was explained by growth in continuous light. Although light induces stomatal opening, keeping the plants in continuous light for 3-4 weeks likely caused the stomata to adjust to the lack of dark periods by reducing stomatal aperture size. Most importantly, the closure of both WS wild-type and R2-4A mutant stomata after 24 h darkness confirms that R2-4A stomata opens more than WS wild-type stomata after 5 h light.

Chapter 6: Conclusions

In the identification of a putative purinoceptor-like receptor, the approach of radiolabeling outside-out enriched plasma membrane proteins was unsuccessful. Though spots were observed on the autoradiogram, indicating that the label $8N_3ATP[\alpha^{32}P]$ successfully bound to plasma membrane proteins, a large number of proteins were sequenced within the corresponding excised gel. As a result, it could not be deciphered which protein bound to the isotope to produce the autoradiogram spot and therefore bound ATP.

Though a receptor was not identified, the experiments described in this thesis produced useful information to guide future investigations. Viewing the proteins sequenced, most are known to be plasma membrane associated. Exceptions were inconsistently sequenced and are abundant in plant cells (e.g., RUBISCO). Therefore, the plasma membrane isolation used was successful. However, due to the sequencing of a large number of cytosol-facing proteins, it is possible that the labeled plasma membrane vesicles were not as enriched for outside-out vesicles as desired. As all plasma membrane proteins were loaded on the 2-D gel, it is also possible that these cytosol-facing proteins ran to the same location as extracellular matrix (ECM) facing labeled proteins and that vesicles were indeed outside-out enriched.

Attempts to label peripheral membrane proteins and integral membrane proteins separately support that most of the proteins binding $8N_3ATP[\alpha^{32}P]$ are peripheral

membrane proteins. Still, autoradiogram spots were observed in both the soluble and insoluble fractions, and a purinoceptor-like receptor could exist in either state.

To continue this biochemical approach to identifying a purinoceptor-like receptor, it is important to reduce the unique proteins run on the 2-D gel or to obtain better protein separation. One approach that has been considered is the use of affinity chromatography using a biotinylated ATP that could be trapped on an avidin column. Using a new approach such as this, it is also important to ensure the purity of enriched outside-out vesicles. Though using a known, well-cited protocol to enrich outside-out vesicles (Larsson et al. 1994), the procedure is complicated and no evidence was obtained to confirm that the plasma membrane proteins labeled here were ECM-facing.

This thesis also included evidence to show that AtAPY1 and AtAPY2 are expressed in guard cells. Comparison of RNA and protein between enriched guard cell protoplasts (high guard cell to mesophyll cell ratio) and whole leaves (low guard cell to mesophyll cell ratio) showed a greater abundance of these apyrases in guard cells compared to mesophyll cells. Though the responsiveness of these guard cell protoplasts to ABA (a stress hormone) has been examined and confirmed (Pandey et al. 2002), it is possible that the protoplasting itself is responsible for upregulation of apyrases. Thus it is important to show that protoplasting does not upregulate APY1 and APY2 expression. Future experiments are needed to test this possibility by comparing apyrase expression in mesophyll cell protoplasts and guard cell protoplasts.

Evidence was also presented revealing a role for APY1 and APY2 in stomatal regulation. Complete suppression of *APY2* and partial suppression (RNAi) of *APY1*

caused stomata to be more open than the WS wild-type after 5 h light. This result was unexpected considering the hypothesized role of APY1 and APY2 to regulate eATP in guard cells and preliminary evidence that indicates higher concentrations of eATP induce stomatal closure. It is important to expand on these results and continue examining the effects of APY inhibitors and antibodies on stomatal regulation, but dissimilar results would not necessarily contradict the results presented here. If the hypothesized role of APY1 and APY2 is correct, it may be that the partial suppression of apyrases in guard cells results in a concentration of eATP optimal for stomatal opening. The data presented here does not provide enough information to determine if stomata open faster during the suppression of *APY1* and *APY2* or if stomata in these mutants have a larger maximum opening. To answer this question, average stomatal aperture in response to longer light treatments than 5 h should be determined.

The effects of 2 h ABA treatment after 3 h light on apyrase suppressed mutants (R2-4A) and the WS wild-type was also described here. ABA caused the same percent closure when apyrase was suppressed as in the WS wild-type but was not as closed as WS after 2 h ABA. This difference can be explained by apyrase suppression resisting the effects of ABA or could be the result of R2-4A stomata starting at a more open state than WS wild-type after a light treatment. In order to determine if ABA can cause closure in R2-4A as equal to WS wild-type, longer treatment times with ABA should be examined.

Though many studies are still required, the results in this thesis provide evidence for an exciting new role for AtAPY1 and AtAPY2 in stomatal regulation. Considering other plant tissues where the function of eATP and these two apyrases are linked, the

evidence presented here also suggests a possible role for the poorly understood signaling agonist, eATP, in guard cell signaling.

References

Abbracchio, M., Burnstock, G., Boeynaems, J-M., Barnard, E., Boyer, J., Kennedy, C., Knight, G., Fumagalli, M., Gachet, C., Jacobson, K., and Weisman, G. (2006). International Union of Pharmacology LVIII: Update on the P2Y G protein-coupled nucleotide receptors: from molecular mechanisms and pathophysiology to therapy. *Pharmacological Reviews* 58: 281-341.

Anderson, L. and Anderson, N. (1977). High resolution two-dimensional electrophoresis of human plasma proteins. *Proc. Natl. Acad. Sci.* 74: 5421-5425.

Alexandersson, E., Saalbach, G., Larsson, C., and Kjellbom, P. (2004). *Arabidopsis* plasma membrane proteomics identifies components of transport, signal transduction, and membrane trafficking. *Plant Cell Physiol.* 45(11): 1543-1556.

Buchthal, F. and Kahlson, G. (1944). The action of adenosine triphosphate and related compounds on mammalian skeletal muscle. *Acta Physiologica Scandinavica* 8(4): 317-324.

Buchthal, F., and Engbaek, L. (1947). Application of adenosine triphosphate and related compounds to the spinal cord of the cat. *J. Physiol.* 106(1): 3.

Burnstock , G., Campbell, D., Satchell, D., and Smythe, A. (1970). Evidence that adenosine triphosphate or a related nucleotide is the transmitter substance released by non-adrenergic inhibitory nerves in the gut. *Br. J. Pharmac.* 40: 668-688.

Burnstock, G. (1972). Purinergic nerves. *Pharmacol. Rev.* 24(3): 509-581.

Burnstock, G. (1980). Purinergic nerves and receptors. *Prog. Biochem. Pharmacol.* 16: 141-154.

Burnstock, G., and Kennedy, C. (1985). Is there a basis for distinguishing two types of P2 purinoceptor? *Gen. Pharmacol.* 16: 433-440.

Butterfield, T. (2007). "The effects of extracellular ATP on growth in *Arabidopsis thaliana*." MA thesis. University of Texas at Austin.

Charest, R., Blackmore, P., and Exton, J. (1985). Characterization of responses of isolated rat hepatocytes to ATP and ADP. *Journal of Biological Chemistry* 260(29): 5789-5794.

Chivasa, S., Ndimba, B., Simon, W., Lindsey, K., and Slabas, A. (2005). Extracellular ATP functions as an endogenous external metabolite regulating plant cell viability. *The Plant Cell* 17: 3019-3034.

Clark, G., Dauwalder, M., and Roux, S. (1992). Purification and immunolocalization of an annexin-like protein in pea seedlings. *Planta* 187: 1-9.

Clark, G., Torres, J., Finlayson, S., Guan, X., Handley, C., Lee, J., Kays, J., Chen, J., and S. Roux. (2010a). Apyrase (nucleoside triphosphate-diphosphohydrolase) and extracellular nucleotides regulate cotton fiber elongation in cultured ovules. *Plant Physiology* 152: 1073-1083.

Clark, G., Wu, M., Wat, N., Onyirimba, J., Pham, T., Herz, N., Ogoti, J., Gomez, D., Canales, A., Aranda, G., Blizard, M., Nyberg, T., Terry, A., Torres, J., Wu, J., and Roux, S. (2010b). Both the stimulation and inhibition of root hair growth induced by extracellular nucleotides in *Arabidopsis* are mediated by nitric oxide and reactive oxygen species. *Plant Molecular Biology* 74: 423-435.

Demidchik, V., Nichols, C., Oliynyk, M., Dark, A., Glover, B., and Davies, J. (2003). Is ATP a signaling agent in plants? *Plant Physiology* 133: 456-461.

Desikan, R., Griffiths, R., Hancock, J., and Neill, S. (2002). A new role for an enzyme: nitrate reductase-mediated nitric oxide generation is required for abscisic acid-induced stomatal closure in *Arabidopsis thaliana*. *Proc. Natl. Acad. Sci.* 99(25): 16314-16318.

Drury, A. and Szent-Gyorgyi, A. (1929). The physiological activity of adenine compounds with especial reference to their action upon the mammalian heart. *J. Physiology-London* 68: 213-237.

Foresi, N., Laxalt, A., Tonón, C., Casalongué, C., and Lamattina, L. (2007). Extracellular ATP induces nitric oxide production in tomato cell suspensions. *Plant Physiology* 145: 589-592.

Fountain, S., Cao, L., Young, M., and North, R. A. (2008). Permeation properties of a P2X receptor in the green algae *Ostreococcus tauri*. *The Jounral of Biological Chemistry* 283(22): 15122-15126.

García-Mata, C. and Lamattina, L. (2001). Nitric oxide induces stomatal closure and enhances the adaptive plant responses against drought stress. *Plant Physiology* 126: 1196-1204.

Grove, M., Spencer, G., and Rohwedder, W. (1979). Brassinolide, a plant growth-promoting steroid isolated from *Brassica napus* pollen. *Nature* 281: 216-217.

Handa, M. and Guidotti, G. (1996). Purification and cloning of a soluble ATP-diphosphohydrolase (apyrase) from potato tubers (*Solanum tuberosum)*. *Biochemical and Biophysical Research Communications* 218: 916-923.

Jaffe, M. (1973). The role of ATP in mechanically stimulated rapid closure of the Venus's-Flytrap. *Plant Physiology* 51: 17-18.

Jeter, C., Tang, W., Henaff, E., Butterfield, T., and Roux, S. (2004). Evidence of a novel cell signaling role for extracellular adenosine triphosphates and diphosphates in *Arabidopsis*. *The Plant Cell* 16: 2652-2664.

Johnson, K., Jones, B., Bacic, A., and Schultz, C. (2003). The fasciclin-like arabinogalactan proteins of *Arabidopsis*. A multigene family of putative cell adhesion molecules. *Plant Physiology* 133: 1911-1925.

Kawate, T., Michel, J., Birdsong, W., and Gouaux, E. (2009). Crystal structure of the ATP-gated $P2X_4$ ion channel in the closed state. *Nature* 460: 592-599

Kim, S-H., Yang, S., Kim, T-J., Han, J-S., and Suh, J-W. (2009). Hypertonic stress increased extracellular ATP levels and the expression of stress-responsive genes in *Arabidopsis thaliana* seedlings. *Biosci. Biotechnol. Biochem.* 73(6): 1252-1256.

Kim, S-Y., Sivaguru, M., and Stacey, G. (2006). Extracellular ATP in plants. Visualization, localization, and analysis of physiological significance in growth and signaling. *Plant Physiology* 142: 984-992.

Kogl, F. and Haagen-Smit, A. J. (1931). "Uber die Chemie des Wuchsstoffs K. Akad. Wetenschap. Amsterdam." *Proc. Sect. Sci.* 34: 1411-1416.

Komoszyński, M. and Wojtczak, A. (1996). Apyrases (ATP diphosphohydrolases, EC 3.6.1.5): function and relationship to ATPases. *Biochimica et Biophysica Acta* 1310: 233-241.

Larsson, C., Sommarin, M., and Widell, S. (1994). Isolation of highly purified plasma membranes and the separation of inside-out and right-side-out vesicles. *Methods Enzymol* 228: 451-469.

Lüttge, U., Schöch, E., and Ball, E. (1974). Can externally applied ATP supply energy to active ion uptake mechanisms of intact plant cells? *Australian Journal of Plant Physiology* 1(2): 211-220.

Ma, A., Bell, D., Mittal, A., and Harrison, H. (1994). Immunocytochemical detection of extracellular annexin II in cultured human skin keratinocytes and isolation of annexin II isoforms enriched in the extracellular pool. *Journal of Cell Science* 107: 1973-1984.

McAinsh, M., Brownlee, C., and Hethering, A. (1990). Calcium ions as second messengers in guard cell signal transduction. *Physiologia Plantarum* 100: 16--29.

McAinsh, M., Clayton, H., Mansfield, T., and Hetherington, A. (1996). Changes in stomatal behavior and guard cell cytosolic free calcium in response to oxidative stress. *Plant Physiology* 111: 1031-1042.

Melotto, M., **Underwood, W., Koczan, J., Nomura, K., and He, S.** Plant stomata function in innate immunity against bacterial invasion. *Cell* 126(5): 969-980.

Mitchell, C. (2001). Release of ATP by a human retinal pigment epithelial cell line: potential for autocrine stimulation through subretinal space. *J Physiol.* 534: 193-202.

Neill, S., Desikan, R., Clarke, A., Hurst, R., and Hancock, J. (2002). Hydrogen peroxide and nitric oxide as signalling molecules in plants. *Journal of Experimental Botany* 53(372): 1237-1247.

Neill, S., Barros, R., Bright, J., Desikan, R., Hancock, J., Harrison, J., Morris, P., Ribeiro, D., and Wilson, I. (2008). Nitric oxide, stomatal closure, and abiotic stress. *Journal of Experimental Botany* 59(2): 165-176.

Nejidat, A., Chanan, I., and Roth-Bejerano, N. (1983). Stomatal response to ATP mediated by phytochrome. *Physiologia Plantarum* 57(3): 367-370.

North, A. (2002). Molecular physiology of P2X receptors. *Physiol. Rev.* 82: 1013-1067.

Otterhag, L., Sommarin, M., and Pical, C. (2001). N-terminal EF-hand-like domain is required for phosphoinositide-specific phospholipase C activity in *Arabidopsis thaliana*. *FEBS Letters* 497: 165-170.

Pandey, S., Wang, X., Coursol, S. and Assmann, S. (2002). Preparation and applications of *Arabidopsis thaliana* guard cell protoplasts. *New Phytologist* 153(3): 517-526.

Pandey, S., Nelson, D., and Assmann, S. (2009). Two novel GPCR-type G proteins are abscisic acid receptors in *Arabidopsis*. *Cell* 136: 136-148.

Pei, Z-M., Kuchitsu, K., Ward, J., Schwarz, M., and Schroeder, J. (1997). Differential abscisic acid regulation of guard cell slow anion channels in *Arabidopsis* wild-type and *abi1* and *abi2* mutants. *The Plant Cell* 9: 409-423.

Pei, Z-M., Murata, Y., Benning, G., Thomine, S., Klüsener, B., Allen, G., Grill, E., and Schroeder, J. (2000). Calcium channels activated by hydrogen peroxide mediate abscisic acid signalling in guard cells. *Nature* 406: 731-734.

Peterman, T. K., Ohol, Y., McReynolds, L., and Luna, E. (2004). Patellin1, a novel Sec14-like protein, localizes to the cell plate and binds phosphoinositides. *Plant Physiology* 136: 3080-3094.

Reichler, S., Torres, J., Rivera, A., Cintolesi, V., Clark, G., and Roux, S. (2009). Intersection of two signalling pathways: extracellular nucleotides regulate pollen germination and pollen tube growth via nitric oxide. *Journal of Experimental Botany* 60(7): 2129-2138.

Romanello, M., Pani, B., Bicego, M., and D'Andrea, P. (2001). Mechanically induced ATP release from human osteoblastic cells. *Biochemical and Biophysical Research Communications* 289(5): 1275-1281.

Schroeder, J., Raschke, K., and Neher, E. (1987). Voltage dependence of K^+ channels in guard-cell protoplasts. *Proc. Natl. Acad. Sci.* 84: 4108-4112.

Schroeder, J. and Hagiwara, S. (1989). Cytosolic calcium regulates ion channels in the plasma membrane of *Vicia faba* guard cells. *Nature* 338: 427-430.

Shope, J., DeWald, D., and Mott, K. (2003). Changes in surface area of intact guard cells are correlated with membrane internalization. *Plant Physiology* 133: 1314-1321.

Song, C., Steinebrunner, I., Wang, X., Stout, S., and Roux, S. (2006). Extracellular ATP induces the accumulation of superoxide via NADPH oxidases in *Arabidopsis*. *Plant Physiology* 140: 1222-1232.

Steinebrunner, I., Wu, J., Sun, Y., Corbett, A., and Roux, S. (2003). Disruption of apyrases inhibits pollen germination in *Arabidopsis*. *Plant Physiology* 131: 1638-1647.

Tang, W., Brady, S., Sun, Y., Muday, G., and Roux, S. (2003). Extracellular ATP inhibits root gravitropism at concentrations that inhibit polar auxin transport. *Plant Physiology* 131: 147-154.

Thomas, C., Rajagopal, A., Windsor, B., Dudler, R., Lloyd, A., and Roux, S. (2000). A role for ectophosphatase in Xenobiotic resistance. *The Plant Cell* 12: 519-533.

Wang, X-Q., Hemayet, U., Jones, A., and Assmann, S. (2001). G protein regulation of ion channels and abscisic acid signalling in *Arabidopsis* guard cells. *Science* 292: 2070-2072.

Wolf, C., Hennig, M., Romanovicz, D., and Steinebrunner, I. (2007). Developmental defects and seedling lethality in apyrase *AtAPY1*and *AtAPY2* double knockout mutants. *Plant Molecular Biology* 64: 657-672.

Wu, J., Steinebrunner, I., Sun, Y., Butterfield, T., Torres, J., Arnold, D., Gonzalez, A., Jacob, F., Reichler, S., and Roux, S. (2007). Apyrases (nucleoside triphosphate-diphosphohydrolases) play a key role in growth control in *Arabidopsis*. *Plant Physiology* 144: 961-975.

Wu, S-J., and Wu, J-Y. (2008). Extracellular ATP-induced NO production and its dependence on membrane Ca^{2+} flux in *Salvia miltiorrhiza* hairy roots. *Journal of Experimental Botany* 59(14): 4007-4016.

Yoo, S., Cho, Y., and Sheen, J. (2007). *Arabidopsis* mesophyll protoplasts: a versatile cell system for transient gene expression analysis. *Nature Protocols* 2(7): 1565-1572.

Zimmerman, H. (2001). Ectonucleotidases: some recent developments and a note on nomenclature. *Drug Development Research* 52: 44-56.

VITA

Devin Scott Fraley was born in Evanston, Illinois and moved to Gilbert, Arizona in the summer of 1998. After completing his work in May 2004 at Mesquite High School, Gilbert, Arizona, he entered Arizona State University in Tempe, Arizona. Enrolled in full-time coursework and employed part-time, he received his degree of Bachelor of Science from Arizona State University in December 2008. During the following months, he was employed as a college tutor until entering the Graduate School at The University of Texas at Austin in August 2008.

Permanent Address: 9807 N FM 620 #19206
Austin, Texas 78726

This thesis was typed by the author.